



MOX–Report No. 39/2011

**Schwarz methods for a preconditioned WOPSIP
method for elliptic problems**

ANTONIETTI, P.F.; AYUSO DE DIOS, B.; BRENNER, S.C.;
SUNG, L.-Y.

MOX, Dipartimento di Matematica “F. Brioschi”
Politecnico di Milano, Via Bonardi 9 - 20133 Milano (Italy)

mox@mate.polimi.it

<http://mox.polimi.it>

Schwarz methods for a preconditioned WOPSIP method for elliptic problems

Paola F. Antonietti*

*MOX–Laboratory for Modeling and Scientific Computing, Dipartimento di Matematica
Piazza Leonardo da Vinci 32, 20133 Milano, Italy*

Blanca Ayuso de Dios†

*Centre de Recerca Matemàtica
Campus de Bellaterra, 08193 Bellaterra (Barcelona), Spain*

Susanne C. Brenner‡

*Department of Mathematics and Center for Computation & Technology
Louisiana State University, Baton Rouge, LA 70803*

Li-yeng Sung§

*Department of Mathematics and Center for Computation & Technology
Louisiana State University, Baton Rouge, LA 70803*

November 19, 2011

Abstract

We construct and analyze non-overlapping Schwarz methods for a preconditioned weakly over-penalized symmetric interior penalty (WOPSIP) method for elliptic problems.

1 Introduction

The weakly over-penalized symmetric interior penalty (WOPSIP) method was introduced in [10] (and extended to higher order elements in [11]) for the Poisson problem: find $u \in H^2(\Omega) \cap H_0^1(\Omega)$ such that

$$\begin{aligned} -\Delta u &= f && \text{in } \Omega, \\ u &= 0 && \text{in } \partial\Omega, \end{aligned} \tag{1}$$

were $\Omega \subset \mathbb{R}^2$ is a polygonal domain and f a given source term in $L^2(\Omega)$. The WOPSIP method is stable for any positive penalty parameter and satisfies quasi-optimal error estimates in both the energy and the L^2 norms. Moreover, its simplicity renders the method particularly suitable for parallel computations (cf. [8]). However, due to the over-penalization, the condition number of the stiffness matrix is of order $O(h^{-4})$, h being the mesh-size. A simple block preconditioner was proposed in [10] that reduces the condition number of the preconditioned system to $O(h^{-2})$. A nice feature of the preconditioner is that by construction it is well suited for parallel computations since it retains the intrinsic parallelism of the

*paola.antonietti@polimi.it

†bayuso@crm.cat

‡brenner@math.lsu.edu

§sung@math.lsu.edu

WOPSIP method. The goal of this paper is to further improve the performance of the preconditioned WOPSIP method and to develop additive Schwarz methods for the resulting preconditioned WOPSIP approximation, without destroying the parallel properties of the final linear algebraic system. We note that overlapping additive Schwarz preconditioners for the unpreconditioned WOPSIP method were investigated in [6], where the condition number of the subdomain problems remain $O(h^{-4})$.

An outline of the paper is as follows. In the next section, we recall the preconditioned WOPSIP discretization for the Poisson problem. Then, we introduce the Schwarz methods for the preconditioned WOPSIP discretization and discuss some computational issues. The convergence analysis is carried out in Section 4 and validated through numerical experiments in Section 5. Finally, the proof of some technical results needed in our theoretical analysis is shown in the Appendix.

Throughout the paper, we shall use standard notation for Sobolev spaces (cf. [1]), and $x \lesssim y$ will mean that there exists a generic constant $C > 0$ (that may not be the same at different occurrences but is always mesh independent) so that $x \leq C y$. Analogously, $x \approx y$ will mean that $C^{-1} y \leq x \leq C y$, for a constant $C > 0$.

2 Problem setting and WOPSIP discretization

In this section, we introduce some notation, recall the WOPSIP approximation and present some of the properties of the formulation.

Let $\{\mathcal{T}_h\}_{h>0}$ be a family of quasi-uniform triangulations of Ω . The mesh size is defined by $h := \max_{T \in \mathcal{T}_h} \text{diam } T$. We denote by V_h the first order discontinuous finite element space associated with \mathcal{T}_h , defined by

$$V_h := \{v \in L^2(\Omega) : v|_T \in \mathbb{P}^1(T) \quad \forall T \in \mathcal{T}_h\},$$

where $\mathbb{P}^1(T)$ is the space of linear polynomials in T . The set of all the edges in \mathcal{T}_h is denoted by \mathcal{E}_h ; the set of internal edges by \mathcal{E}_h° and the set of boundary edges by \mathcal{E}_h^∂ , so that $\mathcal{E}_h := \mathcal{E}_h^\circ \cup \mathcal{E}_h^\partial$. For any $e \in \mathcal{E}_h$, h_e will denote the length of the edge e .

We use standard notation for trace operators [4] to define the jumps $[[v]]$, $[[\boldsymbol{\tau}]]$ and averages $\{\{v\}\}$, $\{\{\boldsymbol{\tau}\}\}$ of (sufficiently regular) scalar and vector-valued functions v and $\boldsymbol{\tau}$. For each interior edge $e \in \mathcal{E}_h^\circ$ such that $e = \partial T^+ \cap \partial T^-$ we define

$$\begin{aligned} [[v]] &:= v_e^+ \mathbf{n}_e^+ + v_e^- \mathbf{n}_e^-, & [[\boldsymbol{\tau}]] &:= \boldsymbol{\tau}_e^+ \cdot \mathbf{n}_e^+ + \boldsymbol{\tau}_e^- \cdot \mathbf{n}_e^-, \\ \{\{v\}\} &:= (v_e^+ + v_e^-)/2, & \{\{\boldsymbol{\tau}\}\} &:= (\boldsymbol{\tau}_e^+ + \boldsymbol{\tau}_e^-)/2, \end{aligned}$$

where v_e^+ (respectively v_e^-) denotes the trace of v on e taken within the interior of T^+ (respectively T^-), and \mathbf{n}_e^+ (respectively \mathbf{n}_e^-) is the unit normal of e pointing towards the outside of T^+ (respectively T^-). For $e \in \mathcal{E}_h^\partial$, we define

$$\{\{\boldsymbol{\tau}\}\} := \boldsymbol{\tau}_e, \quad [[v]] := v_e \mathbf{n}.$$

We do not need either $[[\boldsymbol{\tau}]]$ or $\{\{v\}\}$ on boundary edges, and we leave them undefined.

The WOPSIP approximation to the solution of (1) reads: Find $u_h \in V_h$ such that

$$\mathcal{A}_h(u_h, v) = \int_{\Omega} f v \, dx \quad \forall v \in V_h, \quad (2)$$

where $\mathcal{A}_h(\cdot, \cdot) : V_h \times V_h \rightarrow \mathbb{R}$ is the bilinear form defined by [10, 8]:

$$\mathcal{A}_h(w, v) := \sum_{T \in \mathcal{T}_h} \int_T \nabla w \cdot \nabla v \, dx + \sum_{e \in \mathcal{E}_h} \frac{\alpha}{h_e^3} \int_e \Pi_e^0([[w]]) \cdot \Pi_e^0([[v]]) \, ds \quad \forall w, v \in V_h, \quad (3)$$

Here, α denotes the penalty parameter which we assume to be ≥ 1 and $\Pi_e^0 : L^2(e) \rightarrow \mathbb{P}^0(e)$ is the L^2 -orthogonal projection onto the space $\mathbb{P}^0(e)$ of constant functions on e :

$$\Pi_e^0(v) := \frac{1}{h_e} \int_e v \, ds = v(m_e) \quad \forall e \in \mathcal{E}_h \quad \forall v \in V_h, \quad (4)$$

where in the last step we have used the midpoint rule for integration and m_e is the midpoint of the edge $e \in \mathcal{E}_h$. For vector valued functions $\Pi_e^0(\cdot)$ is defined componentwise.

By considering the energy norm:

$$\|v\|_h^2 := \sum_{T \in \mathcal{T}_h} \|\nabla v\|_{0,T}^2 + \sum_{e \in \mathcal{E}_h} \frac{1}{h_e^3} \|\Pi_e^0([v])\|_{0,e}^2 \quad \forall v \in V_h,$$

(observe that $\|v\|_h^2 = \mathcal{A}_h(v, v)$ for $\alpha = 1$), it can be shown that the bilinear form defining the WOPSIP method is coercive and continuous in V_h :

$$\begin{aligned} \mathcal{A}_h(v, v) &\geq \|v\|_h^2 && \forall v \in V_h, \\ \mathcal{A}_h(v, w) &\lesssim \|v\|_h \|w\|_h && \forall v, w \in V_h. \end{aligned}$$

Also, optimal rates of convergence in the $\|\cdot\|_h$ and L^2 -norms can be proved for the WOPSIP approximation to problem (1) (i.e., the solution of (2)). For details see [9, 10].

2.1 An efficient preconditioner for the WOPSIP method

We recall that, given a basis of V_h , any function $v \in V_h$ is uniquely determined by a set of degrees of freedom (dofs). If \mathbb{A}_h is the stiffness matrix associated with the bilinear form $\mathcal{A}_h(\cdot, \cdot)$ and the given basis, problem (2) can be rewritten as the linear system of equations

$$\mathbb{A}_h \mathbf{u} = \mathbf{f},$$

with \mathbb{A}_h symmetric and positive definite. Due to the over-penalization of the method, it can be easily seen that the condition number of \mathbb{A}_h is of order $\kappa(\mathbb{A}_h) = O(h^{-4})$. To effectively compute the approximation with the WOPSIP method, the bilinear form

$$\mathcal{B}_h(w, v) := \sum_{T \in \mathcal{T}_h} \sum_{e \subset \partial T} w_T(m_e) v_T(m_e) + \sum_{e \in \mathcal{E}_h} \frac{\alpha}{h_e^3} \int_e \Pi_e^0([w]) \cdot \Pi_e^0([v]) \, ds \quad \forall w, v \in V_h,$$

was introduced in [10], where $w_T := w|_T$ for all $T \in \mathcal{T}_h$. Denoting by \mathbb{B}_h the matrix associated to the above bilinear form and the given basis, the authors proved in [10] that

$$\mathbf{v}^T \mathbb{B}_h \mathbf{v} \lesssim \mathbf{v}^T \mathbb{A}_h \mathbf{v} \lesssim h^{-2} \mathbf{v}^T \mathbb{B}_h \mathbf{v} \quad \forall \mathbf{v} \in \mathbb{R}^n, \quad (5)$$

where $n := \dim(V_h)$. From (5), it immediately follows that

$$\kappa(\mathbb{B}_h^{-1} \mathbb{A}_h) = O(h^{-2}).$$

The issue of the efficiency of the preconditioner \mathbb{B}_h was further explored in [8], where the authors showed that if a suitable ordering of the dofs is employed the resulting matrix \mathbb{B}_h (and so its action) turns out to be block diagonal with 1×1 and 2×2 blocks and therefore can be computed in parallel.

The aim of this paper is to design a Schwarz method for the efficient solution of the linear system

$$\mathbb{B}_h^{-1} \mathbb{A}_h \mathbf{u} = \mathbb{B}_h^{-1} \mathbf{f}.$$

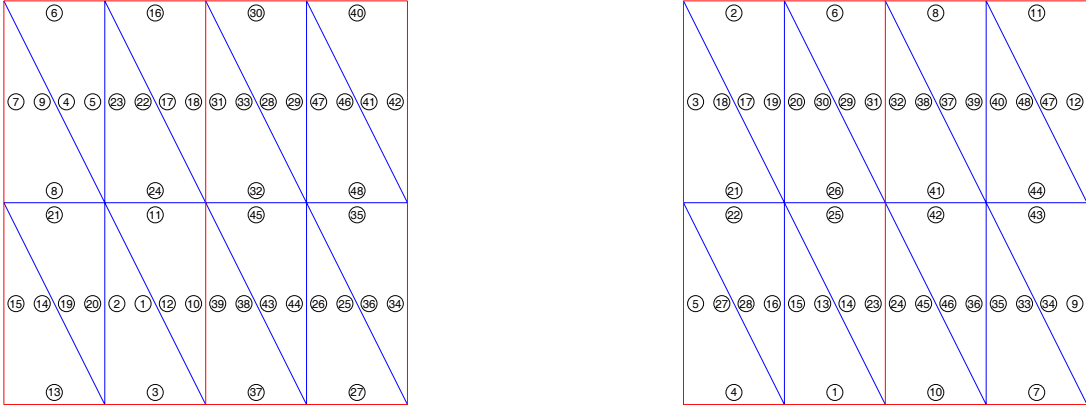


Figure 1: Sample of elementwise (left) and edgewise (right) ordering of the degrees of freedom.

Note that, although \mathbb{A}_h is a symmetric and positive definite (s.p.d.) matrix, $\mathbb{B}_h^{-1}\mathbb{A}_h$ is no longer symmetric in general. Hence, to avoid the non-symmetry and the resulting difficulties, we consider the equivalent linear system of equations

$$\mathbb{D}_h \mathbf{y} = \mathbb{B}_h^{-1/2} \mathbf{f}, \quad (6)$$

where $\mathbf{y} := \mathbb{B}_h^{-1/2} \mathbf{u}$ and

$$\mathbb{D}_h := \mathbb{B}_h^{-1/2} \mathbb{A}_h \mathbb{B}_h^{-1/2},$$

which is well-defined since \mathbb{B}_h is s.p.d. and so it admits a unique s.p.d. square root $\mathbb{B}_h^{1/2}$. From now on, we focus on the construction of Schwarz preconditioners for s.p.d. system of equations (6). Clearly, it still holds that

$$\kappa(\mathbb{B}_h^{-1/2} \mathbb{A}_h \mathbb{B}_h^{-1/2}) = O(h^{-2}),$$

since we can take $\mathbf{v} = \mathbb{B}_h^{-1/2} \mathbf{w}$ in (5) for any $\mathbf{w} \in \mathbb{R}^n$.

So far, we have not said anything about the selection of the basis or the location of the dofs of V_h . In [8], it was shown that the use of the Crouziex-Raviart basis for $\mathbb{P}^1(T)$ on each $T \in \mathcal{T}_h$ and the choice of the dofs at the midpoints of the edges in each T has some advantages. More precisely, the authors showed that by using an edgewise ordering of dofs (that is, the dofs associated to the midpoints of an interior edge are always consecutive, cf. Figure 1 for an example), the matrix \mathbb{B}_h , and consequently \mathbb{B}_h^{-1} , turn out to be block diagonal with 1×1 and 2×2 blocks, and therefore the preconditioned WOPSIP method has an intrinsic highly parallel structure. In the next section we show that by using the same special ordering, also the action of $\mathbb{B}_h^{-1/2}$ retains the same highly parallel structure and can be efficiently computed. Moreover, we shall also show that this ordering facilitates our analysis of the Schwarz methods for the preconditioned WOPSIP discretization. Hence, throughout the rest of the paper it is assumed that the edgewise ordering is employed (see Section 3.2 for details on the implementation).

2.2 Construction of $\mathbb{B}_h^{-1/2}$

As shown in [8], by ordering the dofs in an edgewise manner (cf. Figure 1 (right)) the matrix representing \mathbb{B}_h is block diagonal, with either 2×2 blocks (corresponding to an interior edge) or 1×1 blocks (corresponding to a boundary edge). Denoting by \mathbb{B}_h^e the block of the matrix \mathbb{B}_h corresponding

to the dofs associated to the edge $e \in \mathcal{E}_h$, we have

$$\mathbb{B}_h^e = \begin{cases} \frac{1}{\theta_e} \begin{bmatrix} 1 + \theta_e & -1 \\ -1 & 1 + \theta_e \end{bmatrix} & \text{if } e \in \mathcal{E}_h^\circ, \\ \frac{1}{\theta_e} [1 + \theta_e] & \text{if } e \in \mathcal{E}_h^\partial, \end{cases}$$

where $\theta_e = h_e^2/\alpha$ for all edges $e \in \mathcal{E}_h$. Observe that for any $e \in \mathcal{E}_h^\circ$, since \mathbb{B}_h^e is s.p.d. it can be diagonalized as follows:

$$\mathbb{B}_h^e = \frac{1}{2} \mathbb{Q} \Lambda \mathbb{Q}^T = \frac{1}{2} \begin{bmatrix} 1 & 1 \\ 1 & -1 \end{bmatrix} \cdot \begin{bmatrix} 1 & 0 \\ 0 & \frac{2+\theta_e}{\theta_e} \end{bmatrix} \cdot \begin{bmatrix} 1 & 1 \\ 1 & -1 \end{bmatrix}.$$

And so, we obtain an explicit expression for $(\mathbb{B}_h^e)^{-1/2}$,

$$(\mathbb{B}_h^e)^{-1/2} = \frac{1}{2} \mathbb{Q} \Lambda^{-1/2} \mathbb{Q}^T = \frac{1}{2} \begin{bmatrix} 1 & 1 \\ 1 & -1 \end{bmatrix} \cdot \begin{bmatrix} 1 & 0 \\ 0 & \sqrt{\frac{\theta_e}{2+\theta_e}} \end{bmatrix} \cdot \begin{bmatrix} 1 & 1 \\ 1 & -1 \end{bmatrix} = \frac{1}{2} \begin{bmatrix} 1 + \beta_e & 1 - \beta_e \\ 1 - \beta_e & 1 + \beta_e \end{bmatrix}, \quad (7)$$

where we have set

$$\beta_e := \sqrt{\frac{\theta_e}{2 + \theta_e}} \quad \forall e \in \mathcal{E}_h^\circ.$$

For $e \in \mathcal{E}_h^\partial$, we simply have

$$(\mathbb{B}_h^e)^{-1/2} = [\beta_e^\partial], \quad \beta_e^\partial := \sqrt{\frac{\theta_e}{1 + \theta_e}} \quad \forall e \in \mathcal{E}_h^\partial.$$

We define $\beta := \{\beta_e\}_{e \in \mathcal{E}_h^\circ} \cup \{\beta_e^\partial\}_{e \in \mathcal{E}_h^\partial}$ with

$$\beta|_e := \begin{cases} \beta_e := \sqrt{\frac{\theta_e}{2 + \theta_e}} & \text{if } e \in \mathcal{E}_h^\circ, \\ \beta_e^\partial := \sqrt{\frac{\theta_e}{1 + \theta_e}} & \text{if } e \in \mathcal{E}_h^\partial, \end{cases} \quad \theta_e := \frac{h_e^2}{\alpha} \quad \forall e \in \mathcal{E}_h. \quad (8)$$

Observe now that

$$(\beta|_e)^2 \frac{\alpha}{h_e^3} = \begin{cases} \frac{\alpha}{h_e} \left(\frac{1}{\alpha + h_e^2} \right) \leq \frac{1}{h_e} & \text{if } e \in \mathcal{E}_h^\circ, \\ \frac{\alpha}{h_e} \left(\frac{1}{2\alpha + h_e^2} \right) \leq \frac{1}{2h_e} & \text{if } e \in \mathcal{E}_h^\partial, \end{cases} \quad (9)$$

since $2\alpha + h_e^2 \geq \alpha + h_e^2 > \alpha$. Furthermore, rewriting (8) as $\beta_e^2 = \frac{(\theta_e/k)}{1 + \frac{\theta_e}{k}}$, with $k = 1$ (resp. 2) if e is a boundary (resp. an interior) edge, and assuming that $\theta_e/k \ll 1$, we have

$$\beta_e^2 = \frac{\theta_e}{k} \sum_{i=0}^{\infty} \left(-\frac{\theta_e}{k} \right)^i = \frac{\theta_e}{k} \left(1 + O\left(\frac{\theta_e}{k}\right) \right),$$

and therefore, by using $\theta_e = h_e^2/\alpha$, we obtain

$$\beta_e \approx \frac{h_e}{\sqrt{\alpha}} (1 + O(h_e/\sqrt{\alpha})),$$

and hence, by the quasi-uniformity of the mesh,

$$\beta \approx \frac{h}{\sqrt{\alpha}} (1 + O(h)). \quad (10)$$

Having found an explicit expression for each block $(\mathbb{B}_h^e)^{-1/2}$, we look at its action on the vector of degrees of freedom associated to an edge $e \in \mathcal{E}_h$. Let $e \in \mathcal{E}_h^\circ$ be an arbitrary edge shared by the elements T^+ and T^- , $e = T^+ \cap T^-$, and let $\mathbf{u}_e := [u^+, u^-]^T$ denote the nodal values of the trace $u|_e$ of u at the midpoint of the edge e . It follows from (7) that

$$(\mathbb{B}_h^e)^{-1/2} \mathbf{u}_e = \begin{bmatrix} \{u\} + \beta_e \frac{\mathbf{n}_e^+}{2} \cdot [u] \\ \{u\} - \beta_e \frac{\mathbf{n}_e^-}{2} \cdot [u] \end{bmatrix}.$$

If $e \in \mathcal{E}_h^\partial$ is a boundary edge, we have

$$(\mathbb{B}_h^e)^{-1/2} \mathbf{u}_e = \left[\sqrt{\frac{\theta_e}{1+\theta_e}} \right] \mathbf{u}_e = \beta_e^\partial \mathbf{u}_e.$$

Next, we define the discrete operator $\mathbf{B}_h : V_h \rightarrow V_h'$ associated with the bilinear form $\mathcal{B}_h(\cdot, \cdot)$:

$$\langle \mathbf{B}_h w, v \rangle := \mathcal{B}_h(w, v) \quad \forall w, v \in V_h,$$

where $\langle \cdot, \cdot \rangle$ is the canonical bilinear form. Since the bilinear form $\mathcal{B}_h(\cdot, \cdot)$ is symmetric and coercive, we can define the operator $\mathbf{B}_h^{-1/2} : V_h \rightarrow V_h$. According to the previous discussion, for any $u \in V_h$, $\mathbf{B}_h^{-1/2} u$ is given by

$$(\mathbf{B}_h^{-1/2} u)|_e = \begin{cases} \{u\} + \beta_e \frac{\mathbf{n}_e^+}{2} \cdot [u] & \text{on } T^+ \cap e \\ \{u\} - \beta_e \frac{\mathbf{n}_e^-}{2} \cdot [u] & \text{on } T^- \cap e \end{cases} \quad \forall e \in \mathcal{E}_h^\circ, \quad (11)$$

$$(\mathbf{B}_h^{-1/2} u)|_e = \beta_e^\partial u|_e \quad \forall e \in \mathcal{E}_h^\partial. \quad (12)$$

Finally, we introduce the bilinear form $\mathcal{D}_h(\cdot, \cdot) : V_h \times V_h \rightarrow \mathbb{R}$ defined by

$$\begin{aligned} \mathcal{D}_h(u, v) := \mathcal{A}_h(\mathbf{B}_h^{-1/2} u, \mathbf{B}_h^{-1/2} v) &= \sum_{T \in \mathcal{T}_h} \int_T \nabla(\mathbf{B}_h^{-1/2} u) \cdot \nabla(\mathbf{B}_h^{-1/2} v) \, dx \\ &+ \sum_{e \in \mathcal{E}_h} \frac{\alpha}{h_e^3} \int_e \Pi_e^0(\llbracket \mathbf{B}_h^{-1/2} u \rrbracket) \cdot \Pi_e^0(\llbracket \mathbf{B}_h^{-1/2} v \rrbracket) \, ds, \end{aligned} \quad (13)$$

and the norm

$$\|u\|_{\text{DG}}^2 := \sum_{T \in \mathcal{T}_h} \|\nabla u\|_{0,T}^2 + \sum_{e \in \mathcal{E}_h} \frac{1}{h_e} \|\Pi_e^0(\llbracket u \rrbracket)\|_{0,e}^2 \quad \forall u \in V_h. \quad (14)$$

The next result shows that $\mathcal{D}_h(\cdot, \cdot)$ is continuous and coercive in V_h with respect to the above DG norm, provided h is small enough (see Remark 2.2).

Lemma 2.1. *The bilinear form $\mathcal{D}_h(\cdot, \cdot)$ defined by (13) is continuous in the DG norm (14), and it is also coercive for all $h \leq h_0$ with*

$$h_0 := \min \left(\frac{1}{\sqrt{2}}, \sqrt{\frac{2\alpha}{16C_t^2 - 1}} \right), \quad (15)$$

where C_t is the trace inequality constant. More precisely, there exist $C_c, C_s > 0$ such that

$$\text{Continuity:} \quad \mathcal{D}_h(u, w) \leq C_c \|u\|_{\text{DG}} \|w\|_{\text{DG}} \quad \forall u, w \in V_h; \quad (16)$$

$$\text{Coercivity:} \quad \mathcal{D}_h(u, u) \geq C_s \|u\|_{\text{DG}}^2 \quad \forall u \in V_h. \quad (17)$$

The proof of Lemma 2.1 can be found in Appendix A.

We also define the following bilinear forms

$$\begin{aligned} \mathcal{S}_h(\cdot, \cdot) : V_h \times V_h &\longrightarrow \mathbb{R}, \quad \mathcal{S}_h(w, v) := \sum_{T \in \mathcal{T}_h} \int_T \nabla w \cdot \nabla v \, dx + \sum_{e \in \mathcal{E}_h} \frac{\alpha}{h_e} \int_e \llbracket w \rrbracket \cdot \llbracket v \rrbracket \, ds, \\ \mathcal{S}_h^*(\cdot, \cdot) : V_h \times V_h &\longrightarrow \mathbb{R}, \quad \mathcal{S}_h^*(w, v) := \sum_{T \in \mathcal{T}_h} \int_T \nabla w \cdot \nabla v \, dx + \sum_{e \in \mathcal{E}_h} \frac{\alpha}{h_e} \int_e \Pi_e^0(\llbracket w \rrbracket) \cdot \Pi_e^0(\llbracket v \rrbracket) \, ds. \end{aligned} \tag{18}$$

Remark 2.2. *The restriction on h in Lemma 2.1 is necessary for guaranteeing the coercivity in the DG norm $\|\cdot\|_{DG}$. Note however that taking into account our assumption $\alpha \geq 1$ together with the fact that for piecewise linear polynomials on triangles $C_i^2 \approx 3$ (see for instance [17]), the above restriction on h is a very mild one.*

Remark 2.3. *Notice that since $\mathcal{D}_h(\cdot, \cdot)$ is symmetric, Lemma 2.1 implies in particular that $\mathcal{D}_h(\cdot, \cdot)$, $\mathcal{S}_h(\cdot, \cdot)$ and $\mathcal{S}_h^*(\cdot, \cdot)$ are spectrally equivalent.*

3 Schwarz methods for the preconditioned WOPSIP discretization

In this section we introduce the Schwarz methods and provide some technical tools needed in the analysis.

We denote by \mathcal{T}_N a partition of Ω into N non-overlapping subdomains, i.e., $\Omega = \bigcup_{i=1}^N \Omega_i$, and by $\{\mathcal{T}_H\}_{H>0}$ and $\{\mathcal{T}_h\}_{h>0}$ two families of coarse and fine partitions, respectively, with mesh sizes $H > 0$ and $h > 0$. All the partitions are assumed to be regular and quasi-uniform and we shall always proceed under the assumption that $\mathcal{T}_h, \mathcal{T}_H$ and \mathcal{T}_N are nested:

$$\mathcal{T}_N \subseteq \mathcal{T}_H \subseteq \mathcal{T}_h,$$

i.e., each Ω_i , $i = 1, \dots, N$, can be written as the union of some elements $D \in \mathcal{T}_H$, each of which is the union of elements of the finer partition \mathcal{T}_h ; that is

$$D = \bigcup_{\substack{T_i \in \mathcal{T}_h \\ T_i \subset D}} T_i \quad \forall D \in \mathcal{T}_H.$$

For each subdomain $\Omega_i \in \mathcal{T}_N$, $i = 1, \dots, N$, we define the local DG spaces V_h^i as

$$V_h^i := \{u \in L^2(\Omega_i) : v|_T \in \mathbb{P}^1(T) \quad \forall T \in \mathcal{T}_h, T \subset \Omega_i\},$$

and denote by $\mathbf{R}_i^T : V_h^i \longrightarrow V_h$ the standard inclusion operator from V_h^i to V_h , and by \mathbf{R}_i its transpose with respect to the canonical bilinear form. We observe that

$$V_h = \mathbf{R}_1^T V_h^1 \oplus \dots \oplus \mathbf{R}_N^T V_h^N.$$

Finally, we define

$$\Gamma := \bigcup_{i,j=1}^N \Gamma_{ij} \quad \Gamma_{ij} := \{e \in \mathcal{E}_h, \text{ such that } e \subset \partial\Omega_i \cap \partial\Omega_j, i \neq j\}. \tag{19}$$

We now introduce the *local solvers*, for which we consider two classes: *exact* local solvers (as those proposed in [15]) and *inexact* local solvers (as those introduced in [2, 3]).

(i) **Exact local solvers:** For each subdomain $\Omega_i \in \mathcal{T}_N$, $i = 1, \dots, N$, the local bilinear form $\mathcal{D}_i^E(\cdot, \cdot) : V_h^i \times V_h^i \rightarrow \mathbb{R}$ is defined as the restriction of the (preconditioned) WOPSIP bilinear form (13) to the space $\mathbf{R}_i^T V_h^i$:

$$\mathcal{D}_i^E(u_i, v_i) := \mathcal{D}_h(\mathbf{R}_i^T u_i, \mathbf{R}_i^T v_i) = \mathcal{A}_h(\mathbf{B}_h^{-1/2} \mathbf{R}_i^T u_i, \mathbf{B}_h^{-1/2} \mathbf{R}_i^T v_i) \quad \forall u_i, v_i \in V_h^i. \quad (20)$$

(ii) **Inexact local solvers:** Following [2], we first consider the model problem (1) set in the subdomain Ω_i :

$$-\Delta u_i = f|_{\Omega_i} \quad \text{in } \Omega_i, \quad u_i = 0 \quad \text{on } \partial\Omega_i. \quad (21)$$

The i^{th} -local solver (that is associated to the subdomain Ω_i) is defined as the (preconditioned) WOPSIP approximation to (21). Hence, the local bilinear form $\mathcal{D}_i^I(\cdot, \cdot) : V_h^i \times V_h^i \rightarrow \mathbb{R}$ is given by:

$$\mathcal{D}_i^I(u_i, v_i) := \mathcal{A}_i(\mathbf{B}_i^{-1/2} u_i, \mathbf{B}_i^{-1/2} v_i) \quad \forall u_i, v_i \in V_h^i, \quad (22)$$

where $\mathcal{A}_i(\cdot, \cdot)$ is given by:

$$\mathcal{A}_i(w_i, v_i) := \sum_{\substack{T \in \mathcal{T}_h \\ T \subset \Omega_i}} \int_T \nabla w_i \cdot \nabla v_i \, dx + \sum_{\substack{e \in \mathcal{E}_h \\ e \subset \bar{\Omega}_i}} \frac{\alpha}{h_e^3} \int_e \Pi_e^0(\llbracket w_i \rrbracket) \cdot \Pi_e^0(\llbracket v_i \rrbracket) \, ds. \quad (23)$$

and $\mathbf{B}_i : V_h^i \rightarrow (V_h^i)'$ refers to the operator associated to the bilinear form $\mathcal{B}_i(\cdot, \cdot)$ defined by

$$\mathcal{B}_i(w_i, v_i) := \sum_{\substack{T \in \mathcal{T}_h \\ T \subset \Omega_i}} \sum_{e \subset \partial T} w_{i_T}(m_e) v_{i_T}(m_e) + \sum_{\substack{e \in \mathcal{E}_h \\ e \subset \bar{\Omega}_i}} \frac{\alpha}{h_e^3} \int_e \Pi_e^0(\llbracket w_i \rrbracket) \cdot \Pi_e^0(\llbracket v_i \rrbracket) \, ds \quad \forall w_i, v_i \in V_h^i.$$

Note that, the edges $e \in \mathcal{E}_h^\circ$ such that $e \subset \partial\Omega_i$ although interior edges in the global partition \mathcal{T}_h , are however *boundary* edges with respect to the local partitioning induced in the subdomain Ω_i . On these edges the definition of the jump operator on boundary edges applies, i.e., $\llbracket w_i \rrbracket = w_i|_e \mathbf{n}$. Consequently the action of $\mathbf{B}_i^{-1/2}$ on the functions restricted to these edges is given by (12).

A key issue in the analysis of the non-overlapping Schwarz methods is the relation between the global bilinear form $\mathcal{D}_h(\cdot, \cdot)$ and the sum of the local solvers. To study such a relation, we need first to introduce some additional notation. Recalling the definition (19) of the interface Γ , we define the *strip* Ω_Γ as

$$\Omega_\Gamma = \bigcup_{i,j=1}^N \Omega_{\Gamma_{ij}}, \quad \Omega_{\Gamma_{ij}} = \{T \in \mathcal{T}_h \mid T \text{ has one edge in } \Gamma_{ij}\}. \quad (24)$$

Now following [15, 2] we have the following result:

Lemma 3.1. *For any $u \in V_h$, let $u_i \in V_h^i$, $i = 1, \dots, N$, be the unique functions such that $u = \sum_{i=1}^N \mathbf{R}_i^T u_i$. Then the following identities hold:*

$$\mathcal{D}_h(u, u) = \sum_{i=1}^N \mathcal{D}_i^E(u_i, u_i) + I_h^E(u, u), \quad (25)$$

$$\mathcal{D}_h(u, u) = \sum_{i=1}^N \mathcal{D}_i^I(u_i, u_i) + I_h^I(u, u), \quad (26)$$

where

$$I_h^E(u, u) = 2 \left[\sum_{T \in \Omega_\Gamma} \int_T \nabla(\mathbf{B}_h^{-1/2} \mathbf{R}_i^T u_i) \cdot \nabla(\mathbf{B}_h^{-1/2} \mathbf{R}_j^T u_j) \, dx - \sum_{e \in \Gamma} \beta_e^2 \frac{\alpha}{h_e^3} \int_e \Pi_e^0(u_i) \Pi_e^0(u_j) \, ds \right], \quad (27)$$

$$I_h^I(u, u) = I_h^E(u, u) + G_h^I(u, u), \quad (28)$$

with β_e defined as in (8), and

$$G_h^I(u, u) = \sum_{i=1}^N \left[\sum_{T \in \Omega_T} \int_T \nabla(\mathbf{B}_h^{-1/2} \mathbf{R}_i^T u_i) \cdot \nabla(\mathbf{B}_h^{-1/2} \mathbf{R}_i^T u_i) dx - \sum_{\substack{T \in \Omega_T \\ T \subset \Omega_i}} \int_T \nabla(\mathbf{B}_i^{-1/2} u_i) \cdot \nabla(\mathbf{B}_i^{-1/2} u_i) dx, \right] \\ - \sum_{e \in \Gamma} \frac{\alpha}{h_e^3} \eta_e^2 \int_e ([\Pi_e^0(u_i)]^2 + [\Pi_e^0(u_j)]^2) ds. \quad (29)$$

Here, η_e is defined as:

$$\eta_e^2 := -[\beta_e]^2 + [\beta_e^\partial]^2 = \frac{\theta_e}{(1 + \theta_e)(2 + \theta_e)} > 0, \quad \theta_e = h_e^2/\alpha. \quad (30)$$

Proof. For simplicity we present the proof in the case of $N = 2$ subdomains, that is $\Omega = \Omega_1 \cup \Omega_2$. The extension to the case of N subdomains is straightforward and we omit the details. We first show (25). Taking into account the definition (13) of $\mathcal{D}_h(\cdot, \cdot)$, the linearity and symmetry of $\mathcal{D}_h(\cdot, \cdot)$ and of the exact local solvers $\mathcal{D}_i^E(\cdot, \cdot)$ (cf. (20)), it is easy to see that

$$I_h^E(u, u) = \mathcal{D}_h(u, u) - \mathcal{D}_1^E(u_1, u_1) - \mathcal{D}_2^E(u_2, u_2) = \mathcal{D}_h(\mathbf{R}_1^T u_1, \mathbf{R}_2^T u_2) + \mathcal{D}_h(\mathbf{R}_2^T u_2, \mathbf{R}_1^T u_1) \\ = 2 \mathcal{D}_h(\mathbf{R}_1^T u_1, \mathbf{R}_2^T u_2) \\ = 2 \mathcal{A}_h(\mathbf{B}_h^{-1/2} \mathbf{R}_1^T u_1, \mathbf{B}_h^{-1/2} \mathbf{R}_2^T u_2) \\ = 2 \sum_{T \in \mathcal{T}_h} \int_T \nabla(\mathbf{B}_h^{-1/2} \mathbf{R}_1^T u_1) \cdot \nabla(\mathbf{B}_h^{-1/2} \mathbf{R}_2^T u_2) dx \\ + 2 \sum_{e \in \mathcal{E}_h} \frac{\alpha}{h_e^3} \int_e \Pi_e^0([\mathbf{B}_h^{-1/2} \mathbf{R}_1^T u_1]) \cdot \Pi_e^0([\mathbf{B}_h^{-1/2} \mathbf{R}_2^T u_2]) ds.$$

To give a more explicit expression of the last two terms on the right hand side, we take a closer look at the support of the terms involved. We first observe that $\text{supp}(\mathbf{R}_1^T u_1) \cap \text{supp}(\mathbf{R}_2^T u_2) \subseteq \Gamma$, so it is enough to consider the action of $\mathbf{B}_h^{-1/2}$ on $e \in \Gamma$. Fix an edge $e \in \Gamma$ shared by the elements $T_1 \subseteq \Omega_1$ and $T_2 \subseteq \Omega_2$, and recall that (see Figure 2(a)),

$$\mathbf{R}_1^T u_1 = \begin{cases} u_1 = u|_{\Omega_1} & \text{in } \Omega_1, \\ 0 & \text{in } \Omega_2, \end{cases} \quad \mathbf{R}_2^T u_2 = \begin{cases} 0 & \text{in } \Omega_1, \\ u_2 = u|_{\Omega_2} & \text{in } \Omega_2, \end{cases}$$

Taking into account the action of $\mathbf{B}_h^{-1/2}$ on internal edges (since $e \in \Gamma$ so $e \in \mathcal{E}_h^\circ$) we have

$$(\mathbf{B}_h^{-1/2} \mathbf{R}_1^T u_1)|_e = \mathbf{B}_h^{-1/2} \begin{bmatrix} u_1 \\ 0 \end{bmatrix} = \begin{bmatrix} \frac{1 + \beta_e}{2} u_1 \\ \frac{1 - \beta_e}{2} u_1 \end{bmatrix}, \\ (\mathbf{B}_h^{-1/2} \mathbf{R}_2^T u_2)|_e = \mathbf{B}_h^{-1/2} \begin{bmatrix} 0 \\ u_2 \end{bmatrix} = \begin{bmatrix} \frac{1 - \beta_e}{2} u_2 \\ \frac{1 + \beta_e}{2} u_2 \end{bmatrix}, \quad (31)$$

where β_e is defined as in (8). Therefore, under the action of $\mathbf{B}_h^{-1/2}$, the support of $\mathbf{R}_1^T u_1$ (resp. $\mathbf{R}_2^T u_2$) expands into the Ω_2 (resp. Ω_1) across Γ , with an additional dof at the midpoint of the edge e (see Figure 2(b)). Next, we have to further consider the actions of the operators ∇ and $[\cdot]$ on $\mathbf{B}_h^{-1/2} \mathbf{R}_i^T u_i$.

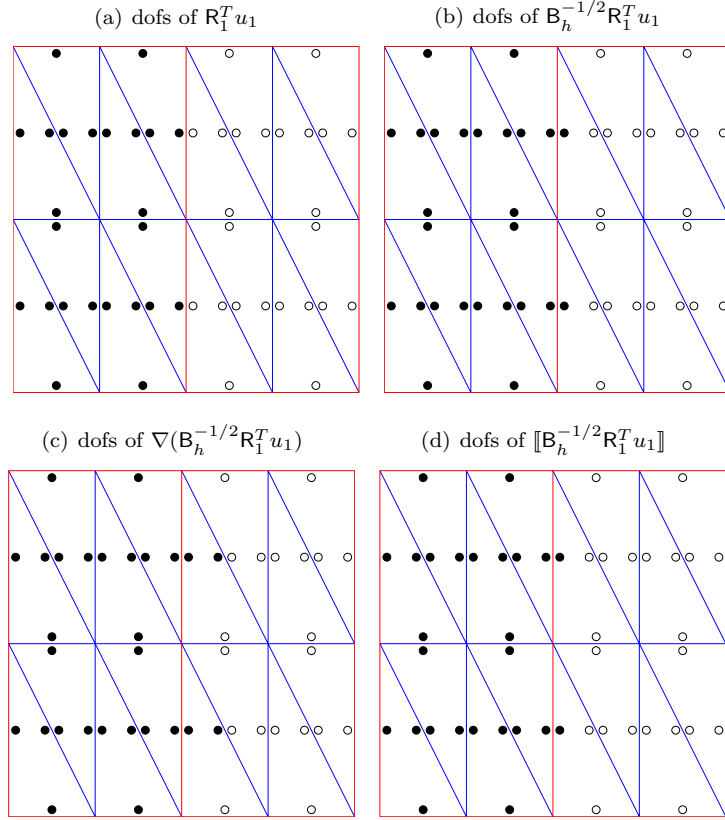


Figure 2: Degrees of freedom of $R_1^T u_1$, $B_h^{-1/2} R_1^T u_1$, $\nabla(B_h^{-1/2} R_1^T u_1)$ and $\llbracket B_h^{-1/2} R_1^T u_1 \rrbracket$, respectively, on a $N = 2$ subdomain partition. The dofs marked with \bullet are different from zero; those marked with \circ are equal to zero.

For the gradient term, it is clear that the resulting support expands along the strip of elements that touch Γ (see Figure 2(c)), that is:

$$\text{supp}(\nabla B_h^{-1/2} R_1^T u_1) \cap \text{supp}(\nabla B_h^{-1/2} R_2^T u_2) \subseteq \Omega_\Gamma, \quad (32)$$

where the set Ω_Γ is defined in (24). For the penalty term, it can be seen that (cf. Figure 2(d)),

$$\text{supp}(\Pi_e^0(\llbracket B_h^{-1/2} R_1^T u_1 \rrbracket)) \cap \text{supp}(\Pi_e^0(\llbracket B_h^{-1/2} R_2^T u_2 \rrbracket)) \subseteq \Gamma. \quad (33)$$

Using the definition of the jump operator on interior edges and (31) we have

$$\llbracket B_h^{-1/2} R_1^T u_1 \rrbracket = \beta_e \llbracket R_1^T u_1 \rrbracket = \beta_e u_1 \mathbf{n}_e^1, \quad \llbracket B_h^{-1/2} R_2^T u_2 \rrbracket = \beta_e \llbracket R_2^T u_2 \rrbracket = \beta_e u_2 \mathbf{n}_e^2, \quad (34)$$

and taking into account the definition (4) we obtain

$$\begin{aligned} \sum_{e \in \Gamma} \frac{\alpha}{h_e^3} \int_e \Pi_e^0(\llbracket B_h^{-1/2} R_1^T u_1 \rrbracket) \cdot \Pi_e^0(\llbracket B_h^{-1/2} R_2^T u_2 \rrbracket) ds &= \sum_{e \in \Gamma} \frac{\alpha}{h_e^2} \llbracket B_h^{-1/2} R_1^T u_1 \rrbracket(m_e) \llbracket B_h^{-1/2} R_2^T u_2 \rrbracket(m_e) \\ &= \sum_{e \in \Gamma} \frac{\alpha}{h_e^2} (\beta_e^2 u_1(m_e) u_2(m_e) \mathbf{n}_e^+ \cdot \mathbf{n}_e^-) = - \sum_{e \in \Gamma} \frac{\alpha}{h_e^3} \beta_e^2 \int_e \Pi_e^0(u_1) \cdot \Pi_e^0(u_2) ds. \end{aligned}$$

Therefore, we finally have

$$I_h^E(u, u) = 2 \left[\sum_{T \in \Omega_\Gamma} \int_T \nabla(\mathbf{B}_h^{-1/2} \mathbf{R}_1^T u_1) \cdot \nabla(\mathbf{B}_h^{-1/2} \mathbf{R}_2^T u_2) \, dx - \sum_{e \in \Gamma} \beta_e^2 \frac{\alpha}{h_e^3} \int_e \Pi_e^0(u_1) \Pi_e^0(u_2) \, ds \right],$$

which establishes (27) and hence (25).

We now turn to the case of *inexact* local solvers and the proof of (26). We first note that, when acting on (the restriction of the functions to) interior edges $e \in \mathcal{E}_h^\circ$ that do not belong to the interface Γ , we have that $\mathbf{B}_h^{-1/2} \equiv \mathbf{B}_i^{-1/2}$. Hence, we can write:

$$I_h^I(u, u) = \mathcal{D}_h(u, u) - \mathcal{D}_1^I(u_1, u_1) - \mathcal{D}_2^I(u_2, u_2) = W_1 + W_2,$$

where

$$W_1 := \sum_{T \in \Omega_\Gamma} \int_T \nabla(\mathbf{B}_h^{-1/2} u) \cdot \nabla(\mathbf{B}_h^{-1/2} u) \, dx - \sum_{i=1}^2 \sum_{\substack{T \in \Omega_\Gamma \\ T \subset \Omega_i}} \int_T \nabla(\mathbf{B}_i^{-1/2} u_i) \cdot \nabla(\mathbf{B}_i^{-1/2} u_i) \, dx,$$

and

$$W_2 := \sum_{e \in \Gamma} \frac{\alpha}{h_e^3} \int_e \left[\Pi_e^0(\llbracket \mathbf{B}_h^{-1/2} u \rrbracket) \cdot \Pi_e^0(\llbracket \mathbf{B}_h^{-1/2} u \rrbracket) - \Pi_e^0(\llbracket \mathbf{B}_1^{-1/2} u_1 \rrbracket) \cdot \Pi_e^0(\llbracket \mathbf{B}_1^{-1/2} u_1 \rrbracket) \right. \\ \left. - \Pi_e^0(\llbracket \mathbf{B}_2^{-1/2} u_2 \rrbracket) \cdot \Pi_e^0(\llbracket \mathbf{B}_2^{-1/2} u_2 \rrbracket) \right] \, ds.$$

We first observe that the main difference with respect to the case of *exact* solvers is that the action of $\mathbf{B}_h^{-1/2}$ on a function restricted to an edge $e \in \Gamma$ differs from the action of the local operator $\mathbf{B}_i^{-1/2}$ entering in the definition of $\mathcal{D}_i^I(\cdot, \cdot)$. In the former case $e \in \Gamma$ is an interior edge, while for the latter e is a boundary edge. In fact, in view of (12) we have

$$\begin{aligned} (\mathbf{B}_1^{-1/2} u_1)|_e &= \mathbf{B}_1^{-1/2} \begin{bmatrix} u_1 \\ 0 \end{bmatrix} = \begin{bmatrix} \beta_e^\partial u_1 \\ 0 \end{bmatrix}, \\ (\mathbf{B}_2^{-1/2} u_2)|_e &= \mathbf{B}_2^{-1/2} \begin{bmatrix} 0 \\ u_2 \end{bmatrix} = \begin{bmatrix} 0 \\ \beta_e^\partial u_2 \end{bmatrix}, \end{aligned} \quad (35)$$

and so in this case the support of $\mathbf{B}_i^{-1/2} u_i$ remains in Ω_i . For W_1 , (32) together with (35) gives

$$W_1 = 2 \sum_{T \in \Omega_\Gamma} \int_T \nabla(\mathbf{B}_h^{-1/2} \mathbf{R}_1^T u_1) \cdot \nabla(\mathbf{B}_h^{-1/2} \mathbf{R}_2^T u_2) \, dx \\ + \sum_{i=1}^2 \left[\sum_{T \in \Omega_\Gamma} \int_T \nabla(\mathbf{B}_h^{-1/2} \mathbf{R}_i^T u_i) \cdot \nabla(\mathbf{B}_h^{-1/2} \mathbf{R}_i^T u_i) \, dx - \sum_{\substack{T \in \Omega_\Gamma \\ T \subset \Omega_i}} \int_T \nabla(\mathbf{B}_i^{-1/2} u_i) \cdot \nabla(\mathbf{B}_i^{-1/2} u_i) \, dx \right]. \quad (36)$$

For the term W_2 , using (35) and (33) we have

$$\llbracket \mathbf{B}_i^{-1/2} u_i \rrbracket = \beta_e^\partial u_i,$$

where β_e^∂ is defined in (8). Hence, taking into account the above identity together with (34) and (33) we find,

$$\Pi_e^0(\llbracket \mathbf{B}_h^{-1/2} u \rrbracket) \cdot \Pi_e^0(\llbracket \mathbf{B}_h^{-1/2} u \rrbracket) = [\beta_e] \left([\Pi_e^0(u_1)]^2 + [\Pi_e^0(u_2)]^2 - 2\Pi_e^0(u_1)\Pi_e^0(u_2) \right),$$

$$\Pi_e^0(\llbracket \mathbf{B}_i^{-1/2} u_i \rrbracket) \cdot \Pi_e^0(\llbracket \mathbf{B}_i^{-1/2} u_i \rrbracket) = [\beta_e^\partial]^2 [\Pi_e^0(u_i)]^2 \quad i = 1, 2.$$

Thus we have

$$\begin{aligned} W_2 &= -2 \sum_{e \in \Gamma} \frac{\alpha}{h_e^3} [\beta_e]^2 \int_e \Pi_e^0(u_1) \Pi_e^0(u_2) \, ds + \sum_{e \in \Gamma} \frac{\alpha}{h_e^3} ([\beta_e]^2 - [\beta_e^\partial]^2) \int_e ([\Pi_e^0(u_1)]^2 + [\Pi_e^0(u_2)]^2) \, ds \\ &= -2 \sum_{e \in \Gamma} \frac{\alpha}{h_e^3} [\beta_e]^2 \int_e \Pi_e^0(u_1) \Pi_e^0(u_2) \, ds - \sum_{e \in \Gamma} \frac{\alpha}{h_e^3} \eta_e^2 \int_e ([\Pi_e^0(u_1)]^2 + [\Pi_e^0(u_2)]^2) \, ds, \end{aligned} \quad (37)$$

where η_e is defined as in (30). Putting together (36) and (37) we finally obtain

$$\begin{aligned} I_h^I(u, u) &= I_h^E(u, u) - \sum_{e \in \Gamma} \frac{\alpha}{h_e^3} \eta_e^2 \int_e ([\Pi_e^0(u_1)]^2 + [\Pi_e^0(u_2)]^2) \, ds \\ &\quad + \sum_{i=1}^2 \left[\sum_{T \in \Omega_\Gamma} \int_T \nabla(\mathbf{B}_h^{-1/2} \mathbf{R}_i^T u_i) \cdot \nabla(\mathbf{B}_h^{-1/2} \mathbf{R}_i^T u_i) \, dx - \sum_{\substack{T \in \Omega_\Gamma \\ T \subset \Omega_i}} \int_T \nabla(\mathbf{B}_i^{-1/2} u_i) \cdot \nabla(\mathbf{B}_i^{-1/2} u_i) \, dx \right], \end{aligned}$$

which is (28), and concludes the proof. \square

The last ingredient in the construction of the Schwarz methods is the *coarse solver*. We consider a coarse partition \mathcal{T}_H and we take for $\ell = 0, 1$

$$V_H \equiv V_h^0 := \{v \in L^2(\Omega) : v|_T \in \mathbb{P}^\ell(T) \quad \forall D \in \mathcal{T}_H\}.$$

We denote by $\mathbf{R}_0^T : V_h^0 \rightarrow V_h$ the standard inclusion operator from V_h^0 to V_h , by \mathbf{R}_0 its transpose with respect to the canonical bilinear forms, and define the following three coarse solvers:

$$\mathcal{D}_0(u_0, v_0) := \mathcal{D}_h(\mathbf{R}_0^T u_0, \mathbf{R}_0^T v_0) \quad \forall u_0, v_0 \in V_h^0, \quad (38)$$

$$\mathcal{S}_0(u_0, v_0) := \mathcal{S}_h(\mathbf{R}_0^T u_0, \mathbf{R}_0^T v_0) \quad \forall u_0, v_0 \in V_h^0, \quad (39)$$

$$\mathcal{S}_0^*(u_0, v_0) := \mathcal{S}_h^*(\mathbf{R}_0^T u_0, \mathbf{R}_0^T v_0) \quad \forall u_0, v_0 \in V_h^0, \quad (40)$$

where $\mathcal{S}_h(\cdot, \cdot), \mathcal{S}_h^*(\cdot, \cdot) : V_h \times V_h \rightarrow \mathbb{R}$ are defined in (18).

Remark 3.2. As in [15, 2], the coarse solver $\mathcal{D}_0(\cdot, \cdot)$ is defined as the restriction of the original method to the coarse finite element space V_h^0 . However, it should be noted that

$$\mathcal{D}_0(u_0, v_0) := \mathcal{D}_h(\mathbf{R}_0^T u_0, \mathbf{R}_0^T v_0) \neq \mathcal{D}_H(u_0, v_0) \quad \forall u_0, v_0 \in V_H.$$

In particular to ensure the performance of the resulting Schwarz method it turns out to be essential to choose the penalty parameter α_H in the definition of $\mathcal{A}_H(\cdot, \cdot)$ as $\alpha_H = \alpha(H/h)^3$.

Remark 3.3. Since the coarse solvers (38), (39) and (40) are defined as the restriction of $\mathcal{D}_h(\cdot, \cdot)$, $\mathcal{S}_h(\cdot, \cdot)$ and $\mathcal{S}_h^*(\cdot, \cdot)$, respectively, to the coarse space V_h^0 , we can immediately conclude that all the coarse solvers are spectrally equivalent thanks to Remark 2.3.

3.1 Schwarz operators

We now define the Schwarz operators and show that they can be viewed as preconditioners for the original (preconditioned) system of equations (6).

For the *exact* local solvers, let $\mathbf{P}_i^E : V_h \rightarrow \mathbf{R}_i^T V_h^i$ be defined as

$$\mathcal{D}_h(\mathbf{P}_i^E u, \mathbf{R}_i^T v_i) := \mathcal{D}_h(u, \mathbf{R}_i^T v_i) = \mathcal{A}_h(\mathbf{B}_h^{-1/2} u, \mathbf{B}_h^{-1/2} \mathbf{R}_i^T v_i) \quad \forall v_i \in V_h^i. \quad (41)$$

For the *inexact* local solvers we set $\mathbf{P}_i^{\mathbb{I}} := \mathbf{R}_i^T \tilde{\mathbf{P}}_i^{\mathbb{I}} : V_h \longrightarrow \mathbf{R}_i^T V_h^i \subset V_h$, where $\tilde{\mathbf{P}}_i^{\mathbb{I}} : V_h \longrightarrow V_h^i$ is defined as

$$\mathcal{D}_i^{\mathbb{I}}(\tilde{\mathbf{P}}_i^{\mathbb{I}} u, v_i) := \mathcal{D}_h(u, \mathbf{R}_i^T v_i) = \mathcal{A}_h(\mathbf{B}_h^{-1/2} u, \mathbf{B}_h^{-1/2} \mathbf{R}_i^T v_i) \quad \forall v_i \in V_h^i. \quad (42)$$

We observe that the operators $\mathbf{P}_i^{\mathbb{E}}$ and $\mathbf{P}_i^{\mathbb{I}}$ are well-defined since the local bilinear forms $\mathcal{D}_i^{\mathbb{E}}(\cdot, \cdot)$ and $\mathcal{D}_i^{\mathbb{I}}(\cdot, \cdot)$ are coercive. We also define the operators $\mathbf{P}_0, \mathbf{Q}_0, \mathbf{T}_0 : V_h \longrightarrow \mathbf{R}_0^T V_h^0$ as follows:

$$\begin{aligned} \mathcal{D}_h(\mathbf{P}_0 u, \mathbf{R}_0^T v_0) &:= \mathcal{D}_h(u, \mathbf{R}_0^T v_0) = \mathcal{A}_h(\mathbf{B}_h^{-1/2} u, \mathbf{B}_h^{-1/2} \mathbf{R}_0^T v_0) \quad \forall v_0 \in V_h^0, \\ \mathcal{S}_h(\mathbf{Q}_0 u, \mathbf{R}_0^T v_0) &:= \mathcal{D}_h(u, \mathbf{R}_0^T v_0) = \mathcal{A}_h(\mathbf{B}_h^{-1/2} u, \mathbf{B}_h^{-1/2} \mathbf{R}_0^T v_0) \quad \forall v_0 \in V_h^0, \\ \mathcal{S}_h^*(\mathbf{T}_0 u, \mathbf{R}_0^T v_0) &:= \mathcal{D}_h(u, \mathbf{R}_0^T v_0) = \mathcal{A}_h(\mathbf{B}_h^{-1/2} u, \mathbf{B}_h^{-1/2} \mathbf{R}_0^T v_0) \quad \forall v_0 \in V_h^0. \end{aligned} \quad (43)$$

Since the coarse bilinear forms $\mathcal{D}_h(\cdot, \cdot)$, $\mathcal{S}_h(\cdot, \cdot)$ and $\mathcal{S}_h^*(\cdot, \cdot)$ are coercive, the operators \mathbf{P}_0 , \mathbf{Q}_0 and \mathbf{T}_0 are well defined.

We are now ready to define the following additive Schwarz operators:

$$\mathbf{P}^{\mathbb{E}} := \sum_{i=1}^N \mathbf{P}_i^{\mathbb{E}} + \mathbf{P}_0, \quad \mathbf{Q}^{\mathbb{E}} := \sum_{i=1}^N \mathbf{P}_i^{\mathbb{E}} + \mathbf{Q}_0, \quad \mathbf{T}^{\mathbb{E}} := \sum_{i=1}^N \mathbf{P}_i^{\mathbb{E}} + \mathbf{T}_0. \quad (44)$$

$$\mathbf{P}^{\mathbb{I}} := \sum_{i=1}^N \mathbf{P}_i^{\mathbb{I}} + \mathbf{P}_0, \quad \mathbf{Q}^{\mathbb{I}} := \sum_{i=1}^N \mathbf{P}_i^{\mathbb{I}} + \mathbf{Q}_0, \quad \mathbf{T}^{\mathbb{I}} := \sum_{i=1}^N \mathbf{P}_i^{\mathbb{I}} + \mathbf{T}_0. \quad (45)$$

In the case of *exact* local solvers, the matrix representation of the additive Schwarz operators $\mathbf{P}^{\mathbb{E}}$, $\mathbf{Q}^{\mathbb{E}}$ and $\mathbf{T}^{\mathbb{E}}$ is given by

$$\begin{aligned} \mathbb{P}^{\mathbb{E}} &= \left(\sum_{i=1}^N \mathbf{R}_i^T (\mathbb{D}_i^{\mathbb{E}})^{-1} \mathbf{R}_i + \mathbf{R}_0^T \mathbb{D}_0^{-1} \mathbf{R}_0 \right) \mathbb{D}_h := \mathbb{M}_1^{\mathbb{E}} \mathbb{D}_h, \\ \mathbb{Q}^{\mathbb{E}} &= \left(\sum_{i=1}^N \mathbf{R}_i^T (\mathbb{D}_i^{\mathbb{E}})^{-1} \mathbf{R}_i + \mathbf{R}_0^T \mathbb{S}_0^{-1} \mathbf{R}_0 \right) \mathbb{D}_h := \mathbb{M}_2^{\mathbb{E}} \mathbb{D}_h, \\ \mathbb{T}^{\mathbb{E}} &= \left(\sum_{i=1}^N \mathbf{R}_i^T (\mathbb{D}_i^{\mathbb{E}})^{-1} \mathbf{R}_i + \mathbf{R}_0^T (\mathbb{S}_0^*)^{-1} \mathbf{R}_0 \right) \mathbb{D}_h := \mathbb{M}_3^{\mathbb{E}} \mathbb{D}_h, \end{aligned}$$

where \mathbb{S}_h and \mathbb{S}_h^* are the matrix representations of the bilinear forms $\mathcal{S}_h(\cdot, \cdot)$ and $\mathcal{S}_h^*(\cdot, \cdot)$, respectively. We observe that the preconditioners differ by the choice of the coarse solver (cf. Table 1). $\mathbb{M}_1^{\mathbb{E}}$ employs as coarse solver the restriction of the preconditioned WOPSIP bilinear form to the finite element coarse space whereas for $\mathbb{M}_2^{\mathbb{E}}$ and $\mathbb{M}_3^{\mathbb{E}}$ the coarse solver is defined as the restriction to the coarse space of the bilinear form $\mathcal{S}_h(\cdot, \cdot)$ and $\mathcal{S}_h^*(\cdot, \cdot)$, respectively. The same kind of representation holds for *inexact* local solvers. Details are given in Table 1.

3.2 Computational issues

Let \mathbf{v} be a vector representing a finite element function v in the edgewise ordering, and let \mathbb{P} be the permutation matrix so that $\mathbb{P}\mathbf{v}$ becomes the vector representing \mathbf{v} in the elementwise ordering. We define \mathbb{J} to be the matrix representing the jumps term

$$\mathbf{w}^T \mathbb{J} \mathbf{v} = \sum_{e \in \mathcal{E}_h} \frac{\alpha}{h_e^3} \int_e \Pi_e^0(\llbracket w \rrbracket) \cdot \Pi_e^0(\llbracket v \rrbracket) \, ds,$$

and \mathbb{G} to be the matrix representing the volume term

$$\mathbf{w}^T \mathbb{G} \mathbf{v} = \sum_{T \in \mathcal{T}_h} \int_T \nabla w \cdot \nabla v \, dx.$$

| Preconditioner | Coarse Component | Local Components ($i = 1, \dots, N$) |
|--|--|--|
| $\mathbb{M}_1^E := \sum_{i=1}^N \mathbf{R}_i^T (\mathbb{D}_i^E)^{-1} \mathbf{R}_i + \mathbf{R}_0^T \mathbb{D}_0^{-1} \mathbf{R}_0$ | $\mathbb{D}_0 := \mathbf{R}_0 \mathbb{D}_h \mathbf{R}_0^T$ | $\mathbb{D}_i^E := \mathbf{R}_i \mathbb{D}_h \mathbf{R}_i^T$ |
| $\mathbb{M}_2^E := \sum_{i=1}^N \mathbf{R}_i^T (\mathbb{D}_i^E)^{-1} \mathbf{R}_i + \mathbf{R}_0^T \mathbb{S}_0^{-1} \mathbf{R}_0$ | $\mathbb{S}_0 := \mathbf{R}_0 \mathbb{S}_h \mathbf{R}_0^T$ | $\mathbb{D}_i^E := \mathbf{R}_i \mathbb{D}_h \mathbf{R}_i^T$ |
| $\mathbb{M}_3^E := \sum_{i=1}^N \mathbf{R}_i^T (\mathbb{D}_i^E)^{-1} \mathbf{R}_i + \mathbf{R}_0^T (\mathbb{S}_0^*)^{-1} \mathbf{R}_0$ | $\mathbb{S}_0^* := \mathbf{R}_0 \mathbb{S}_h^* \mathbf{R}_0^T$ | $\mathbb{D}_i^E := \mathbf{R}_i \mathbb{D}_h \mathbf{R}_i^T$ |
| $\mathbb{M}_1^I := \sum_{i=1}^N \mathbf{R}_i^T (\mathbb{A}_i^I)^{-1} \mathbf{R}_i + \mathbf{R}_0^T \mathbb{D}_0^{-1} \mathbf{R}_0$ | $\mathbb{D}_0 := \mathbf{R}_0 \mathbb{D}_h \mathbf{R}_0^T$ | see (22) |
| $\mathbb{M}_2^I := \sum_{i=1}^N \mathbf{R}_i^T (\mathbb{A}_i^I)^{-1} \mathbf{R}_i + \mathbf{R}_0^T \mathbb{S}_0^{-1} \mathbf{R}_0$ | $\mathbb{S}_0 := \mathbf{R}_0 \mathbb{S}_h \mathbf{R}_0^T$ | see (22) |
| $\mathbb{M}_3^I := \sum_{i=1}^N \mathbf{R}_i^T (\mathbb{A}_i^I)^{-1} \mathbf{R}_i + \mathbf{R}_0^T (\mathbb{S}_0^*)^{-1} \mathbf{R}_0$ | $\mathbb{S}_0^* := \mathbf{R}_0 \mathbb{S}_h^* \mathbf{R}_0^T$ | see (22) |

Table 1: Coarse and local components for the preconditioners $\mathbb{M}_1^E - \mathbb{M}_2^E - \mathbb{M}_3^E$ and $\mathbb{M}_1^I - \mathbb{M}_2^I - \mathbb{M}_3^I$.

We remark that in the elementwise ordering the matrix \mathbb{G} is block diagonal with 3×3 blocks, whereas in the edgewise ordering the matrix \mathbb{J} is block diagonal and therefore the preconditioner $\mathbb{B}_h = \mathbb{I} + \mathbb{J}$ is block diagonal, with \mathbb{I} the identity matrix. Therefore, $\mathbb{B}_h^{-1/2}$ is block diagonal as well and the 2×2 blocks can be computed directly with (7). Algorithm 1 computes the action of the stiffness matrix of the WOPSIP method and the action of the preconditioner $\mathbb{B}_h^{-1/2}$ on a vector (cf. [8]).

Algorithm 1 Compute $\mathbf{z} = \mathbb{B}_h^{-1/2} \mathbb{A}_h \mathbb{B}_h^{-1/2} \mathbf{v}$

Solve $\mathbb{B}_h^{1/2} \mathbf{z} = \mathbf{v}$
 Compute $\mathbf{x} := \mathbb{J} \mathbf{z}$
 Compute $\mathbf{y} := \mathbb{P}^T \mathbb{G} \mathbf{P} \mathbf{z}$
 Solve $\mathbb{B}_h^{1/2} \mathbf{z} = \mathbf{x} + \mathbf{y}$

Next, we also describe the action of the additive Schwarz preconditioner \mathbb{M}_1^E on a vector \mathbf{v} edgewise ordered (cf. Algorithm 2). The routines for the other preconditioners can be written exactly in the same way with only notational changes involved. Note that, for the application of the preconditioner, it is more convenient to employ the elementwise ordering of the dofs, and to number first the dofs corresponding to elements in the first subdomain, then the dofs corresponding to elements in the second subdomain and so on. With such an ordering, the local solvers turn out to be a block Jacobi preconditioner where each block corresponds to the dofs in a subdomain.

Algorithm 2 Compute $\mathbf{z} = \mathbb{M}_1^E \mathbf{v}$

Solve $\mathbf{z} = \mathbf{R}_0^T \mathbb{D}_0^{-1} \mathbf{R}_0^T \mathbb{P} \mathbf{v}$
for $i = 1, \dots, N$ **do**
 $\mathbf{z} \leftarrow \mathbf{z} + \mathbf{R}_i^T \mathbb{D}_i^{-1} \mathbf{R}_i^T \mathbf{z}$
end for
 $\mathbf{z} \leftarrow \mathbb{P}^T \mathbf{z}$.

4 Convergence analysis

In this section we present the convergence analysis of the proposed Schwarz methods for the preconditioned WOPSIP scheme. We start by stating the main result of this section:

Theorem 4.1. *Let \mathcal{P} be any of the Schwarz operators defined in (44) and (45). Then, the condition number of \mathcal{P} satisfies*

$$\kappa(\mathcal{P}) \leq C_0^2 \omega_{\mathbf{r}} (N_a + 1) \lesssim 1 + \frac{H}{h}, \quad \mathbf{r} = \mathbf{E} \text{ or } \mathbf{I},$$

where N_a is the maximum number of adjacent subdomains that a given subdomain might have and $\omega_{\mathbf{r}}$ is a positive constant independent of H, h and the number of subdomains.

The rest of the section is devoted to the proof of the above theorem. We follow the classical abstract convergence theory of Schwarz methods [14, 13] (cf. also [16, Chapter 2] and [12, Chapter 7]), and therefore, we only have to verify the following three *assumptions*.

Assumption A1 (Stable decomposition). *There exists $C_0 > 0$ such that every $u \in V_h$ admits a decomposition $u = \sum_{i=0}^N \mathbf{R}_i^T u_i$, with $u_0 \in V_h^0$, and $u_i \in V_h^i$, $i = 1, \dots, N$, that satisfies*

$$\sum_{i=1}^N \mathcal{D}_i^{\mathbf{r}}(u_i, u_i) + \gamma_0(u_0, u_0) \leq C_0^2 \mathcal{D}_h(u, u), \quad \mathbf{r} = \mathbf{E} \text{ or } \mathbf{I},$$

where $\gamma_0(\cdot, \cdot)$ is one of the coarse bilinear forms defined in (38)–(40).

Assumption A2 (Strengthened Cauchy–Schwarz inequalities). *There exist $0 \leq \varepsilon_{ij} \leq 1$, $1 \leq i, j \leq N$, such that*

$$|\mathcal{D}_h(\mathbf{R}_i^T u_i, \mathbf{R}_j^T u_j)| \leq \varepsilon_{ij} \mathcal{D}_h(\mathbf{R}_i^T u_i, \mathbf{R}_i^T u_i)^{1/2} \mathcal{D}_h(\mathbf{R}_j^T u_j, \mathbf{R}_j^T u_j)^{1/2}$$

for all $v_i \in V_h^i$, $v_j \in V_h^j$. Define $\rho(\mathcal{E})$ to be the spectral radius of $\mathcal{E} := \{\varepsilon_{ij}\}_{i,j=1,\dots,N}$.

Assumption A3 (Local stability). *There exists $\omega_{\mathbf{r}} > 0$ such that*

$$\mathcal{D}_h(\mathbf{R}_i^T u_i, \mathbf{R}_i^T u_i) \leq \omega_{\mathbf{r}} \mathcal{D}_i^{\mathbf{r}}(u_i, u_i) \quad \forall u_i \in V_h^i, \quad \mathbf{r} = \{\mathbf{E}, \mathbf{I}\}. \quad (46)$$

We start by verifying Assumption A2. Following [15, 2], it is straightforward to see that $\varepsilon_{ii} = 1$ for $i = 1, \dots, N$. For $i \neq j$, we note that $\mathcal{D}_h(\mathbf{R}_i^T u_i, \mathbf{R}_j^T u_j) = \mathcal{A}_h(B_i^{-1/2} \mathbf{R}_i^T u_i, B_j^{-1/2} \mathbf{R}_j^T u_j) \neq 0$ only if $\partial\Omega_i \cap \partial\Omega_j \neq \emptyset$, so $\varepsilon_{ij} = 1$ in those cases, and $\varepsilon_{ij} = 0$ otherwise. Then, $\rho(\mathcal{E})$ can be bounded by $\rho(\mathcal{E}) \leq \max_i \sum_j |\varepsilon_{ij}| \leq 1 + N_a$, where N_a is the maximum number of adjacent subdomains that a given subdomain might have.

In the next sections we verify Assumptions A3 and A1.

4.1 Local stability

We now prove that the local solvers satisfy a *local stability* property. Observe that for the *exact* local solvers defined in (20), it follows from their definition that (46) holds true with $\omega_{\mathbf{E}} \equiv 1$. Before showing that Assumption A3 holds true also for the inexact local solvers, we define the norm $\|\cdot\|_{\text{DG}, \Omega_i}$ according to (14) but at the subdomain level, i.e.,

$$\|u_i\|_{\text{DG}, \Omega_i}^2 := \sum_{\substack{T \in \mathcal{T}_h \\ T \subset \Omega_i}} \|\nabla u_i\|_{0,T}^2 + \sum_{\substack{e \in \mathcal{E}_h \\ e \subset \Omega_i}} \frac{1}{h_e} \|\Pi_e^0(\llbracket u_i \rrbracket)\|_{0,e}^2 + \sum_{\substack{e \in \mathcal{E}_h \\ e \subset \partial\Omega_i}} \frac{1}{h_e} \|\Pi_e^0(u_i \mathbf{n})\|_{0,e}^2 \quad \forall u_i \in V_h^i,$$

and observe that the coercivity (17) holds also at the subdomain level for $h \leq h_0$ with h_0 given in (15), by the definition of $\mathcal{D}_i^{\mathbf{r}}(\cdot, \cdot)$.

The next result shows that the local stability property holds also for the inexact local solvers defined in (22).

Lemma 4.2. For $i = 1, \dots, N$, let $\mathcal{D}_i^{\mathbb{I}} : V_h^i \times V_h^i \rightarrow \mathbb{R}$ be the bilinear form defined by (22). Then, there exists $\omega_{\mathbb{I}} > 0$ such that the following local stability property holds:

$$\mathcal{D}_h(\mathbf{R}_i^T u_i, \mathbf{R}_i^T u_i) \leq \omega_{\mathbb{I}} \mathcal{D}_i^{\mathbb{I}}(u_i, u_i) \quad \forall u_i \in V_h^i \quad \forall i = 1, \dots, N.$$

Proof. Observe that

$$\|\mathbf{R}_i^T u_i\|_{\text{DG}}^2 = \|u_i\|_{\text{DG}, \Omega_i}^2.$$

It then follows from (16) and (17) (for $\mathcal{D}_i^{\mathbb{I}}(\cdot, \cdot)$) that

$$\mathcal{D}_h(\mathbf{R}_i^T u_i, \mathbf{R}_i^T u_i) \leq C_c \|\mathbf{R}_i^T u_i\|_{\text{DG}}^2 \leq C_c \|u_i\|_{\text{DG}, \Omega_i}^2 \leq C \mathcal{D}_i^{\mathbb{I}}(u_i, u_i).$$

□

4.2 Stable decomposition

In this section we finally show that the decomposition underlying the definition of the additive Schwarz operator is indeed stable with respect to the energy norm defined by $\mathcal{D}_h(\cdot, \cdot)$.

We first state an auxiliary result needed in the proof of Proposition 4.5. This result provides an estimate for the interface bilinear forms $I_h^{\mathbb{E}}(\cdot, \cdot)$ and $I_h^{\mathbb{I}}(\cdot, \cdot)$.

Lemma 4.3. For any $u \in V_h$, it holds that

$$|I_h^r(u, u)| \lesssim \|u\|_{\text{DG}}^2 + h^{-1} \sum_{D \in \mathcal{T}_H} \sum_{E \subset \partial D} \|u\|_{0,E}^2, \quad r = \mathbb{E} \text{ or } \mathbb{I}. \quad (47)$$

Proof. We start by proving the bound for $I_h^{\mathbb{E}}(\cdot, \cdot)$. From the definition (27) of $I_h^{\mathbb{E}}$ given in Lemma 3.1 and the standard triangle inequality, we have $|I_h^{\mathbb{E}}(u, u)| \leq 2|F_1| + 2|F_2|$, where

$$F_1 := \sum_{T \in \Omega_{\mathbb{I}}} \int_T \nabla(\mathbf{B}_h^{-1/2} \mathbf{R}_i^T u_i) \cdot \nabla(\mathbf{B}_h^{-1/2} \mathbf{R}_j^T u_j) \, dx,$$

$$F_2 := \sum_{e \in \Gamma} \beta_e^2 \frac{\alpha}{h_e^3} \int_e \Pi_e^0(u_i) \Pi_e^0(u_j) \, ds.$$

We next estimate the two terms separately, starting with F_2 . By recalling the definition (8) of β_e on $e \in \mathcal{E}_h^{\circ}$ and using (9), the Cauchy-Schwarz inequality, the arithmetic-geometric inequality and the stability of the projection $\Pi_e^0(\cdot)$, we find

$$\begin{aligned} 2|F_2| &\leq 2 \left(\sum_{e \in \Gamma} \frac{1}{h_e} \|\Pi_e^0(u_i)\|_{0,e}^2 \right)^{1/2} \left(\sum_{e \in \Gamma} \frac{1}{h_e} \|\Pi_e^0(u_j)\|_{0,e}^2 \right)^{1/2} \\ &\leq \sum_{e \in \Gamma} \frac{1}{h_e} \|\Pi_e^0(u_i)\|_{0,e}^2 + \sum_{e \in \Gamma} \frac{1}{h_e} \|\Pi_e^0(u_j)\|_{0,e}^2 \leq \sum_{e \in \Gamma} \left(\frac{1}{h_e} \|u_i\|_{0,e}^2 + \frac{1}{h_e} \|u_j\|_{0,e}^2 \right). \end{aligned}$$

Observe that each subdomain Ω_i is the union of some elements $D \in \mathcal{T}_H$ and the mesh is quasi-uniform. Denoting by E the edges of D , we have

$$2|F_2| \leq \sum_{e \in \Gamma} (h_e^{-1} \|u_i\|_{0,e}^2 + h_e^{-1} \|u_j\|_{0,e}^2) \lesssim h^{-1} \sum_{D \in \mathcal{T}_H} \sum_{E \subset \partial D} \|u\|_{0,E}^2. \quad (48)$$

Next, we estimate the term $|F_1|$. Using the Cauchy-Schwarz inequality we have

$$\begin{aligned} |F_1| &= \left| \sum_{\substack{i,j=1 \\ i \neq j}}^N \sum_{T \in \Omega_{\Gamma_{ij}}} \int_T \nabla(\mathbf{B}_h^{-1/2} \mathbf{R}_i^T u_i) \cdot \nabla(\mathbf{B}_h^{-1/2} \mathbf{R}_j^T u_j) \, dx \right| \\ &\lesssim \sum_{\substack{i,j=1 \\ i \neq j}}^N \left(\sum_{T \in \Omega_{\Gamma_{ij}}} \|\nabla \mathbf{B}_h^{-1/2} \mathbf{R}_i^T u_i\|_{0,T} \|\nabla \mathbf{B}_h^{-1/2} \mathbf{R}_j^T u_j\|_{0,T} \right). \end{aligned} \quad (49)$$

Observe that for any fixed $j \neq i$ and $T \in \Omega_{\Gamma_{ij}}$ with $T \subseteq \Omega_i$, the divergence theorem, the Cauchy-Schwarz and the trace inequalities together with the stability of the projection $\Pi_e^0(\cdot)$ give

$$\begin{aligned} \|\nabla \mathbf{B}_h^{-1/2} \mathbf{R}_j^T u_j\|_{0,T}^2 &= - \int_T \Delta(\mathbf{B}_h^{-1/2} \mathbf{R}_j^T u_j) \mathbf{B}_h^{-1/2} \mathbf{R}_j^T u_j \, dx + \int_{\partial T} \nabla(\mathbf{B}_h^{-1/2} \mathbf{R}_j^T u_j) \cdot \mathbf{n} \mathbf{B}_h^{-1/2} \mathbf{R}_j^T u_j \, ds \\ &= \int_{\partial T} \nabla(\mathbf{B}_h^{-1/2} \mathbf{R}_j^T u_j) \cdot \mathbf{n} \Pi_e^0(\mathbf{B}_h^{-1/2} \mathbf{R}_j^T u_j) \, ds \\ &\leq \|\nabla(\mathbf{B}_h^{-1/2} \mathbf{R}_j^T u_j)\|_{0,\partial T} \|\Pi_e^0(\mathbf{B}_h^{-1/2} \mathbf{R}_j^T u_j)\|_{0,\partial T} \\ &\lesssim \|\nabla(\mathbf{B}_h^{-1/2} \mathbf{R}_j^T u_j)\|_{0,T} h_e^{-1/2} \|\mathbf{R}_j^T u_j\|_{0,e} \quad (e = \partial T \cap \Gamma_{ij}), \end{aligned} \quad (50)$$

where in the last step we have used the fact that $\Pi_e^0(\mathbf{B}_h^{-1/2} \mathbf{R}_j^T u_j) \neq 0$ only on the edge $e = \partial T \cap \Gamma_{ij}$ due to (31) (see also Figure 2) and hence

$$\|\nabla \mathbf{B}_h^{-1/2} \mathbf{R}_j^T u_j\|_{0,T} \lesssim h_e^{-1/2} \|u_j\|_{0,e} \quad e = \partial T \cap \Gamma_{ij} \quad T \subset \Omega_i \cap \Omega_{\Gamma_{ij}} \quad i \neq j.$$

After inserting the estimate (49) into (49) and using the continuity (16) of $\mathcal{D}_h(\cdot, \cdot)$ given in Lemma 2.1, we finally obtain

$$\begin{aligned} |F_1| &\lesssim \sum_{\substack{i,j=1 \\ i \neq j}}^N \left(\sum_{\substack{T \in \Omega_{\Gamma_{ij}} \\ T \subset \Omega_i}} \|\nabla \mathbf{B}_h^{-1/2} \mathbf{R}_i^T u_i\|_{0,T} h_e^{-1/2} \|u_j\|_{0,e} + \sum_{\substack{T \in \Omega_{\Gamma_{ij}} \\ T \subset \Omega_j}} \|\nabla \mathbf{B}_h^{-1/2} \mathbf{R}_i^T u_j\|_{0,T} h_e^{-1/2} \|u_i\|_{0,e} \right) \\ &\hspace{15em} (e = \partial T \cap \Gamma_{ij}) \\ &\lesssim \sum_{T \in \Omega_{\Gamma}} \left(\|\nabla u\|_{0,T}^2 + \sum_{e \subset \partial T} h_e^{-1} \|\Pi_0(\llbracket u \rrbracket)\|_{0,e}^2 \right) + h^{-1} \sum_{D \in \mathcal{T}_H} \sum_{E \subset \partial D} \|u\|_{0,E}^2 \\ &\lesssim \|u\|_{\text{DG}}^2 + h^{-1} \sum_{D \in \mathcal{T}_H} \sum_{E \subset \partial D} \|u\|_{0,E}^2. \end{aligned}$$

The above estimate together with (48) concludes the proof for $I_h^E(\cdot, \cdot)$. To bound $I_h^I(\cdot, \cdot)$ we observe that, thanks to Lemma 3.1

$$I_h^I(u, u) = I_h^E(u, u) + G_h^I(u, u) \quad \forall u \in V_h,$$

and so it is enough to bound $G_h^I(\cdot, \cdot)$ which we recall is defined as

$$G_h^I(u, u) = \sum_{i=1}^N \sum_{T \in \Omega_{\Gamma}} \int_T \nabla(\mathbf{B}_h^{-1/2} \mathbf{R}_i^T u_i) \cdot \nabla(\mathbf{B}_h^{-1/2} \mathbf{R}_i^T u_i) \, dx \quad (F3)$$

$$- \sum_{i=1}^N \sum_{\substack{T \in \Omega_{\Gamma} \\ T \subset \Omega_i}} \int_T \nabla(\mathbf{B}_i^{-1/2} u_i) \cdot \nabla(\mathbf{B}_i^{-1/2} u_i) \, dx \quad (F4)$$

$$- \sum_{i=1}^N \sum_{e \in \Gamma} \frac{\alpha}{h_e^3} \eta_e^2 \int_e ([\Pi_e^0(u_i)]^2 + [\Pi_e^0(u_j)]^2) ds. \quad (F5)$$

We start with the last term F_5 . Recalling the definition (30) of η_e and using the fact that $\alpha^2/(\alpha + h_e^2)(2\alpha + h_e^2) \leq 1$, we have

$$\frac{\alpha}{h_e^3} \eta_e^2 = \frac{\alpha}{h_e^3} \frac{\theta_e}{(1 + \theta_e)(2 + \theta_e)} = \frac{1}{h_e} \frac{\alpha^2}{(\alpha + h_e^2)(2\alpha + h_e^2)} \leq \frac{1}{h_e}.$$

Then, taking into account the stability of the projection $\Pi_e^0(\cdot)$ and arguing as we did for F_2 , we obtain

$$|F_5| \leq \sum_{i=1}^N \sum_{e \in \Gamma} \frac{\alpha}{h_e^3} \eta_e^2 (\|u_i\|_{0,e}^2 + \|u_j\|_{0,e}^2) \lesssim 2 \sum_{i=1}^N \sum_{e \in \Gamma} \frac{1}{h_e} \|u_i\|_{0,e}^2 \lesssim h^{-1} \sum_{D \in \mathcal{T}_H} \sum_{E \subset \partial D} \|u\|_{0,E}^2.$$

We now estimate the other terms. The estimate for F_3 is similar to the estimate for $|F_1|$:

$$\begin{aligned} |F_3| &\leq \sum_{i=1}^N \sum_{\substack{T \in \Omega_\Gamma \\ T \subset \Omega_i}} \|\nabla(\mathbf{B}_h^{-1/2} \mathbf{R}_i^T u_i)\|_{0,T}^2 + \sum_{i=1}^N \sum_{\substack{T \in \Omega_\Gamma \\ T \not\subset \Omega_i}} \|\nabla(\mathbf{B}_h^{-1/2} \mathbf{R}_i^T u_i)\|_{0,T}^2 \\ &\lesssim \sum_{T \in \Omega_\Gamma} \left(\|\nabla u\|_{0,T}^2 + \sum_{e \subset \partial T} h_e^{-1} \|\Pi_0(\llbracket u \rrbracket)\|_{0,e}^2 \right) + h^{-1} \sum_{D \in \mathcal{T}_H} \sum_{E \subset \partial D} \|u\|_{0,E}^2 \\ &\lesssim \|u\|_{\text{DG}}^2 + h^{-1} \sum_{D \in \mathcal{T}_H} \sum_{E \subset \partial D} \|u\|_{0,E}^2. \end{aligned}$$

Finally, the term F_4 is readily estimated by the continuity of the bilinear form $\mathcal{D}_i^{\text{I}}(\cdot, \cdot)$:

$$|F_4| \leq \sum_{i=1}^N \sum_{\substack{T \in \Omega_\Gamma \\ T \subset \Omega_i}} \|\nabla(\mathbf{B}_i^{-1/2} u_i)\|_{0,T}^2 \lesssim \sum_{i=1}^N \|u_i\|_{\text{DG}, \Omega_i}^2 \lesssim \|u\|_{\text{DG}}^2 + h^{-1} \sum_{D \in \mathcal{T}_H} \sum_{E \subset \partial D} \|u\|_{0,E}^2.$$

□

The last preliminary result concerns the coarse solver.

Lemma 4.4. *For any $u \in V_h$, let $u_0 \in V_h^0 = V_H$ be defined as*

$$u_0|_D := \frac{1}{|D|} \int_D u dx \quad \forall D \in \mathcal{T}_H. \quad (51)$$

Then it holds that

$$\gamma_0(u_0, u_0) \lesssim (1 + Hh^{-1}) \mathcal{D}_h(u, u), \quad (52)$$

where $\gamma_0(\cdot, \cdot)$ is one of the coarse bilinear forms defined in (38)–(40).

Proof. It is sufficient to show the bound in the case $\gamma_0(\cdot, \cdot) = \mathcal{S}_0^*(\cdot, \cdot)$; the other two cases follow from the observation made in Remark 3.3. Let $u \in V_h$ and let u_0 be defined as in (51). Note that u_0 is piecewise constant (by definition) on \mathcal{T}_H . Then it follows from the definition of $\mathcal{S}_0^*(\cdot, \cdot)$, adding and subtracting u and the stability of the projection $\Pi^0(\cdot)$ that

$$\mathcal{S}_0^*(u_0, u_0) = \sum_{e \in \mathcal{E}_h} \frac{\alpha}{h_e} \int_e |\Pi_e^0(\llbracket R_0^T u_0 \rrbracket)|^2 ds$$

$$\begin{aligned}
&\lesssim \sum_{e \in \mathcal{E}_h} \frac{1}{h_e} \int_e |\Pi_e^0(\llbracket R_0^T u_0 - u \rrbracket)|^2 ds + \sum_{e \in \mathcal{E}_h} \frac{1}{h_e} \int_e |\Pi_e^0(\llbracket u \rrbracket)|^2 ds \\
&\lesssim \sum_{e \in \mathcal{E}_h} \frac{1}{h_e} \int_e |\llbracket R_0^T u_0 - u \rrbracket|^2 ds + \mathcal{D}_h(u, u),
\end{aligned}$$

where in the last step we have also used the coercivity of $\mathcal{D}_h(\cdot, \cdot)$ (cf. (17)). We now observe that last term can be estimated exactly following [15] and [2, Lemma 4.3]:

$$\sum_{e \in \mathcal{E}_h} \frac{1}{h_e} \int_e |\llbracket R_0^T u_0 - u \rrbracket|^2 ds \lesssim Hh^{-1} \|u\|_{\text{DG}}^2 \lesssim Hh^{-1} \mathcal{D}_h(u, u).$$

□

We close the section with the proof of Assumption A1.

Proposition 4.5 (Stable decomposition). *For any $u \in V_h$, let $u = \sum_{i=0}^N \mathbf{R}_i^T u_i$, $u_i \in V_h^i$, $i = 0, \dots, N$, where $u_0 \in V_h^0$ is defined by*

$$u_0|_D := \frac{1}{|D|} \int_D u dx \quad \forall D \in \mathcal{T}_H,$$

and u_1, \dots, u_N are (uniquely) determined by $u - \mathbf{R}_0^T u_0 = \mathbf{R}_1^T u_1 + \dots + \mathbf{R}_N^T u_N$. Then, there exists $C_0^2 = O(Hh^{-1})$ such that

$$\sum_{i=1}^N \mathcal{D}_i^{\mathbf{r}}(u_i, u_i) + \gamma_0(u_0, u_0) \leq C_0^2 \mathcal{D}_h(u, u), \quad \mathbf{r} = \{\mathbf{E}, \mathbf{I}\},$$

where $\gamma_0(\cdot, \cdot)$ is one of the coarse bilinear forms defined in (38)–(40).

Proof. The proof follows those given in [15, 2]. We set $\gamma_0(\cdot, \cdot) = \mathcal{D}_0(\cdot, \cdot)$. Given $u \in V_h$, we decompose $u - \mathbf{R}_0^T u_0$ uniquely as $\sum_{i=1}^N \mathbf{R}_i^T u_i$. Taking into account Lemma 3.1 we can write

$$\mathcal{D}_0(u_0, u_0) + \sum_{i=1}^N \mathcal{D}_i^{\mathbf{r}}(u_i, u_i) = \mathcal{D}_0(u_0, u_0) + \mathcal{D}_h(u - \mathbf{R}_0^T u_0, u - \mathbf{R}_0^T u_0) - I_h^{\mathbf{r}}(u - \mathbf{R}_0^T u_0, u - \mathbf{R}_0^T u_0), \quad (53)$$

then we just need to estimate each term on the right hand side.

The first term is readily estimated by using Lemma 4.4:

$$\mathcal{D}_0(u_0, u_0) \lesssim (1 + Hh^{-1}) \mathcal{D}_h(u, u). \quad (54)$$

For the second term on the right hand side of (53), triangle inequality, the continuity of $\mathcal{D}_h(\cdot, \cdot)$ (cf. (16)) together with (54) and the definition of the coarse solver gives,

$$\begin{aligned}
\mathcal{D}_h(u - \mathbf{R}_0^T u_0, u - \mathbf{R}_0^T u_0) &\lesssim \mathcal{D}_h(u, u) + \mathcal{D}_h(\mathbf{R}_0^T u_0, \mathbf{R}_0^T u_0) \\
&= \mathcal{D}_h(u, u) + \mathcal{D}_0(u_0, u_0) \lesssim (1 + Hh^{-1}) \mathcal{D}_h(u, u).
\end{aligned} \quad (55)$$

For the last term, it follows from (17), Lemma 4.3 and (55) that

$$\begin{aligned}
|I_h^{\mathbf{r}}(u - \mathbf{R}_0^T u_0, u - \mathbf{R}_0^T u_0)| &\lesssim \|u - \mathbf{R}_0^T u_0\|_{\text{DG}}^2 + \sum_{D \in \mathcal{T}_H} \sum_{E \subset \partial D} h^{-1} \|u - \mathbf{R}_0^T u_0\|_{0,E}^2 \\
&\lesssim (1 + Hh^{-1}) \mathcal{D}_h(u, u) + h^{-1} \sum_{D \in \mathcal{T}_H} \sum_{E \subset \partial D} \|u - \mathbf{R}_0^T u_0\|_{0,E}^2.
\end{aligned}$$

Noting now that the trace inequality together with a Poincaré-Friedrichs inequality [7] gives

$$\begin{aligned} \sum_{D \in \mathcal{T}_H} \sum_{E \subset \partial D} h^{-1} \|u - R_0^\top u_0\|_{0,E}^2 &\lesssim \left[\sum_{D \in \mathcal{T}_H} H_D^{-1} h^{-1} \|u - R_0^\top u_0\|_{0,D}^2 + H_D h^{-1} \|\nabla_h(u - R_0^\top u_0)\|_{0,D}^2 \right] \\ &\lesssim H h^{-1} \|u\|_{\text{DG}}^2 + H h^{-1} \sum_{T \in \mathcal{T}_h} \|\nabla u\|_{0,T}^2 \lesssim H h^{-1} \mathcal{D}_h(u, u), \end{aligned}$$

we finally obtain the estimate

$$|I_h^\top(u - R_0^\top u_0, u - R_0^\top u_0)| \lesssim (1 + H h^{-1}) \mathcal{D}_h(u, u)$$

for the last term in (53). Substituting this estimate together with (55) and (54) into (53), the proof is completed. For the other coarse solvers, the proof follows exactly the same steps, replacing the bound in (54) by the corresponding one. \square

5 Numerical results

In this section we present a series of numerical experiments to highlight the practical performance of our non-overlapping Schwarz preconditioners.

We restrict ourselves to two-dimensional model problems: we let $\Omega = (0, 1) \times (0, 1)$ and choose f such that the analytical solution of the model problem (1) is given by $u(x, y) = \exp(xy)(x - x^2)(y - y^2)$. Throughout Sections 5.1 and 5.2 we take the stability constant α appearing in the formulation of the WOPSIP method (3) to be 1; numerical results with different choices of the penalty parameter are discussed in Section 5.3.

We employ a uniform subdomain partition consisting of $N = 4, 16$ squares, and consider initial coarse and fine refinements as depicted in Figure 3 (for $N = 4$ (top) and $N = 16$ (bottom)). We denote by H_0 and h_0 the corresponding initial coarse and fine mesh sizes, respectively, and consider $j = 1, 2, 3$, successive uniform refinements of the initial grids.

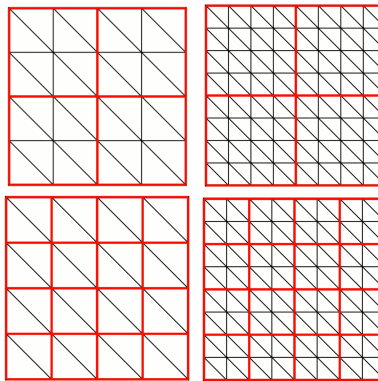


Figure 3: Initial coarse and fine refinements, respectively, on $N = 4$ subdomain partitions (top) and $N = 16$ subdomain partitions.

We solved the preconditioned linear systems of equations by the conjugate gradient (CG) iterative solver with a (relative) tolerance set equal to 10^{-9} allowing a maximum of 100 iterations. For the solution of the linear system (6) we employed the CG iterative solver with the same relative tolerance but allowing a maximum of 1100 iterates.

5.1 Exact local solvers

In this section we test the performance of the Schwarz preconditioners

$$\begin{aligned} \mathbb{M}_1^E &= \sum_{i=1}^N \mathbf{R}_i^T (\mathbb{D}_i^E)^{-1} \mathbf{R}_i + \mathbf{R}_0^T \mathbb{D}_0^{-1} \mathbf{R}_0, \\ \mathbb{M}_2^E &= \sum_{i=1}^N \mathbf{R}_i^T (\mathbb{D}_i^E)^{-1} \mathbf{R}_i + \mathbf{R}_0^T \mathbb{S}_0^{-1} \mathbf{R}_0, \\ \mathbb{M}_3^E &= \sum_{i=1}^N \mathbf{R}_i^T (\mathbb{D}_i^E)^{-1} \mathbf{R}_i + \mathbf{R}_0^T (\mathbb{S}_0^*)^{-1} \mathbf{R}_0, \end{aligned}$$

applied to the original symmetric (preconditioned) systems of equations (6). In the first set of experiments we have considered a coarse space constructed from piecewise linear discontinuous elements. The condition number estimates together with the corresponding iteration counts needed to reach convergence (between parenthesis) for all the considered preconditioners are reported in Table 2 on a partition with 16 subdomains. For the sake of comparison, we also report (last but one row of Table 2) the condition number estimate of the matrix $\mathbb{B}_h^{-1/2} \mathbb{A}_h \mathbb{B}_h^{-1/2}$ together with the iteration counts needed for the solution of the linear system of equations (6). The last row of Table 2 shows the condition

| Preconditioner \mathbb{M}_1^E | | | | |
|--|-----------------|-----------------|-----------------|------------------|
| $H \downarrow h \rightarrow$ | h_0 | $h_0/2$ | $h_0/4$ | $h_0/8$ |
| H_0 | 5.1815 (23) | 5.9422 (25) | 9.0724 (33) | 17.1532 (45) |
| $H_0/2$ | - | 5.2452 (23) | 5.9113 (26) | 8.9409 (33) |
| $H_0/4$ | - | - | 5.3608 (23) | 5.9822 (26) |
| $H_0/8$ | - | - | - | 5.4379 (23) |
| Preconditioner \mathbb{M}_2^E | | | | |
| $H \downarrow h \rightarrow$ | h_0 | $h_0/2$ | $h_0/4$ | $h_0/8$ |
| H_0 | 6.6250 (27) | 7.6977 (30) | 11.6106 (37) | 21.7983 (49) |
| $H_0/2$ | - | 7.5231 (29) | 8.0398 (31) | 11.9791 (39) |
| $H_0/4$ | - | - | 7.9609 (30) | 8.3793 (32) |
| $H_0/8$ | - | - | - | 8.2273 (31) |
| Preconditioner \mathbb{M}_3^E | | | | |
| $H \downarrow h \rightarrow$ | h_0 | $h_0/2$ | $h_0/4$ | $h_0/8$ |
| H_0 | 6.6459 (27) | 7.7096 (30) | 11.6134 (37) | 21.7993 (49) |
| $H_0/2$ | - | 7.5603 (29) | 8.0511 (31) | 11.9826 (39) |
| $H_0/4$ | - | - | 7.9947 (30) | 8.3903 (32) |
| $H_0/8$ | - | - | - | 8.2664 (31) |
| $\mathbb{B}_h^{-1/2} \mathbb{A}_h \mathbb{B}_h^{-1/2}$ | 1.2229e+2 (52) | 4.7212e+2 (100) | 1.8726e+3 (202) | 7.4752e+3 (410) |
| \mathbb{A}_h | 2.5173e+4 (115) | 3.9949e+5 (229) | 6.3800e+6 (486) | 1.0309e+8 (1040) |

Table 2: Preconditioners \mathbb{M}_1^E , \mathbb{M}_2^E and \mathbb{M}_3^E ($N = 16$, $\alpha = 1$): condition number estimates and iteration counts. Piecewise linear discontinuous coarse space.

number and the corresponding iteration counts of the original unpreconditioned system of equations

$\mathbb{A}_h \mathbf{x} = \mathbf{f}$. The numerical results confirm the theoretical estimates provided in Theorem 4.1: the condition number of the preconditioned system behaves asymptotically as H/h , and, consequently, the iteration counts behaves asymptotically as $\sqrt{H/h}$. By a comparison with the computed condition number of the matrix \mathbb{A}_h it is clear that the application of all the preconditioners drastically reduce the condition number of the system, and consequently, the iteration counts needed for convergence.

Next, we investigate the scalability of the preconditioners, i.e., the independence of the performance on the number of subdomains. To this end we repeated the same set of experiments decreasing the number of subdomains from $N = 16$ to $N = 4$: the results are reported in Table 3. As predicted from our theoretical estimates, the condition number of the preconditioned system is independent of the number of subdomains.

| Preconditioner \mathbb{M}_1^E | | | | |
|---------------------------------|-------------|-------------|-------------|--------------|
| $H \downarrow h \rightarrow$ | h_0 | $h_0/2$ | $h_0/4$ | $h_0/8$ |
| H_0 | 4.8722 (21) | 5.7042 (24) | 8.9088 (30) | 16.5838 (40) |
| $H_0/2$ | - | 5.0710 (22) | 5.8873 (25) | 9.0200 (32) |
| $H_0/4$ | - | - | 5.3561 (23) | 5.9792 (26) |
| $H_0/8$ | - | - | - | 5.4471 (23) |

| Preconditioner \mathbb{M}_2^E | | | | |
|---------------------------------|-------------|-------------|--------------|--------------|
| $H \downarrow h \rightarrow$ | h_0 | $h_0/2$ | $h_0/4$ | $h_0/8$ |
| H_0 | 6.8843 (27) | 7.7219 (29) | 11.8249 (37) | 21.5324 (50) |
| $H_0/2$ | - | 7.4641 (29) | 8.2226 (31) | 12.1736 (38) |
| $H_0/4$ | - | - | 8.0459 (30) | 8.4641 (32) |
| $H_0/8$ | - | - | - | 8.2667 (31) |

| Preconditioner \mathbb{M}_3^E | | | | |
|--|-----------------|-----------------|-----------------|------------------|
| $H \downarrow h \rightarrow$ | h_0 | $h_0/2$ | $h_0/4$ | $h_0/8$ |
| H_0 | 6.9179 (27) | 7.7294 (29) | 11.8275 (37) | 21.5322 (50) |
| $H_0/2$ | - | 7.5241 (29) | 8.2336 (31) | 12.1763 (38) |
| $H_0/4$ | - | - | 8.0865 (30) | 8.4768 (32) |
| $H_0/8$ | - | - | - | 8.3095 (31) |
| $\mathbb{B}_h^{-1/2} \mathbb{A}_h \mathbb{B}_h^{-1/2}$ | 1.2229e+2 (52) | 4.7212e+2 (100) | 1.8726e+3 (202) | 7.4752e+3 (410) |
| \mathbb{A}_h | 2.5173e+4 (115) | 3.9949e+5 (229) | 6.3800e+6 (486) | 1.0309e+8 (1040) |

Table 3: Preconditioners \mathbb{M}_1^E , \mathbb{M}_2^E and \mathbb{M}_3^E ($N = 4$, $\alpha = 1$): condition number estimates and iteration counts. Piecewise linear discontinuous coarse space.

Next, we investigate the effect of the coarse space on the performance of our preconditioners. To this end, we ran the same set of experiments as before (on a partition with 16 subdomains) employing a piecewise constant coarse space. Table 4 reports the condition number estimates and the corresponding iteration counts. Note that whenever we employ a piecewise constant coarse space the bilinear forms $\mathcal{S}_h(\cdot, \cdot)$ and $\mathcal{S}_h^*(\cdot, \cdot)$ turn out to be identical, and therefore the preconditioners \mathbb{M}_2^E and \mathbb{M}_3^E coincide. For this reason, in Table 4 we only report the results obtained with the preconditioners \mathbb{M}_1^E and \mathbb{M}_2^E . We observe that the performance of the preconditioners are consistently poorer. On the other hand with this choice of coarse space only one degree of freedom per coarse element is required.

| Preconditioner \mathbb{M}_1^E | | | | |
|---------------------------------|-------------|--------------|--------------|--------------|
| $H \downarrow h \rightarrow$ | h_0 | $h_0/2$ | $h_0/4$ | $h_0/8$ |
| H_0 | 9.1821 (27) | 19.1929 (38) | 39.5807 (50) | 80.6716 (70) |
| $H_0/2$ | - | 10.6855 (31) | 22.1790 (44) | 45.2087 (64) |
| $H_0/4$ | - | - | 11.8751 (36) | 24.4631 (50) |
| $H_0/8$ | - | - | - | 12.7832 (38) |

| Preconditioner \mathbb{M}_2^E | | | | |
|--|-----------------|-----------------|-----------------|------------------|
| $H \downarrow h \rightarrow$ | h_0 | $h_0/2$ | $h_0/4$ | $h_0/8$ |
| H_0 | 9.4006 (29) | 20.2353 (40) | 42.7406 (54) | 88.3442 (76) |
| $H_0/2$ | - | 11.6003 (35) | 23.9082 (48) | 49.1192 (68) |
| $H_0/4$ | - | - | 13.2304 (38) | 26.8473 (55) |
| $H_0/8$ | - | - | - | 14.4078 (41) |
| $\mathbb{B}_h^{-1/2} \mathbb{A}_h \mathbb{B}_h^{-1/2}$ | 1.2229e+2 (52) | 4.7212e+2 (100) | 1.8726e+3 (202) | 7.4752e+3 (410) |
| \mathbb{A}_h | 2.5173e+4 (115) | 3.9949e+5 (229) | 6.3800e+6 (486) | 1.0309e+8 (1040) |

Table 4: Preconditioners \mathbb{M}_1^E and \mathbb{M}_2^E ($N = 16$, $\alpha = 1$): condition number estimates and iteration counts. Piecewise constant discontinuous coarse space.

5.2 Inexact local solvers

In this section we test the performance of the Schwarz preconditioners (with inexact local solvers)

$$\begin{aligned} \mathbb{M}_1^I &= \sum_{i=1}^N \mathbf{R}_i^T (\mathbb{A}_i^I)^{-1} \mathbf{R}_i + \mathbf{R}_0^T \mathbb{D}_0^{-1} \mathbf{R}_0, \\ \mathbb{M}_2^I &= \sum_{i=1}^N \mathbf{R}_i^T (\mathbb{A}_i^I)^{-1} \mathbf{R}_i + \mathbf{R}_0^T \mathbb{S}_0^{-1} \mathbf{R}_0, \\ \mathbb{M}_3^I &= \sum_{i=1}^N \mathbf{R}_i^T (\mathbb{A}_i^I)^{-1} \mathbf{R}_i + \mathbf{R}_0^T (\mathbb{S}_0^*)^{-1} \mathbf{R}_0, \end{aligned}$$

applied to the original symmetric (preconditioned) systems of equations (6).

We ran the same set of experiments as before. More precisely, in Table 5 and Table 6 we compare the condition number estimates and the iteration counts obtained on a subdomain partition made of $N = 16$ and $N = 4$ subdomains, respectively, employing a piecewise linear discontinuous coarse space. As expected, the preconditioners with inexact local solvers are also scalable, and the condition number estimates of the preconditioned system are in agreement with Theorem 4.1: the computed condition number seems to behave as $O(H/h)$.

Finally, we test again the performance of the preconditioners where the coarse spaces are constructed from piecewise constant polynomials. The computed condition number estimates and the corresponding iteration counts obtained by employing the preconditioners \mathbb{M}_1^I and \mathbb{M}_2^I are shown in Table 7. By comparing the results with the analogous ones presented in the previous Section 5.1 it can be inferred that employing exact local solvers improves the performance of the preconditioner slightly.

| Preconditioner M_1^I | | | | |
|------------------------------|-------------|-------------|--------------|--------------|
| $H \downarrow h \rightarrow$ | h_0 | $h_0/2$ | $h_0/4$ | $h_0/8$ |
| H_0 | 4.2990 (21) | 7.3572 (28) | 14.3928 (40) | 29.5718 (57) |
| $H_0/2$ | - | 4.7076 (22) | 7.7532 (30) | 14.4282 (41) |
| $H_0/4$ | - | - | 4.9095 (23) | 8.1509 (30) |
| $H_0/8$ | - | - | - | 5.0121 (23) |

| Preconditioner M_2^I | | | | |
|------------------------------|-------------|-------------|--------------|--------------|
| $H \downarrow h \rightarrow$ | h_0 | $h_0/2$ | $h_0/4$ | $h_0/8$ |
| H_0 | 5.5549 (25) | 9.4431 (32) | 18.7975 (45) | 38.8577 (64) |
| $H_0/2$ | - | 6.2441 (26) | 10.1556 (34) | 18.7271 (47) |
| $H_0/4$ | - | - | 6.5799 (28) | 10.6361 (35) |
| $H_0/8$ | - | - | - | 6.6286 (29) |

| Preconditioner M_3^I | | | | |
|--|-----------------|-----------------|-----------------|------------------|
| $H \downarrow h \rightarrow$ | h_0 | $h_0/2$ | $h_0/4$ | $h_0/8$ |
| H_0 | 5.5855 (25) | 9.4545 (32) | 18.8013 (45) | 38.8591 (64) |
| $H_0/2$ | - | 6.2788 (27) | 10.1688 (35) | 18.7303 (47) |
| $H_0/4$ | - | - | 6.6139 (28) | 10.6507 (35) |
| $H_0/8$ | - | - | - | 6.6689 (29) |
| $\mathbb{B}_h^{-1/2} \mathbb{A}_h \mathbb{B}_h^{-1/2}$ | 1.2229e+2 (52) | 4.7212e+2 (100) | 1.8726e+3 (202) | 7.4752e+3 (410) |
| \mathbb{A}_h | 2.5173e+4 (115) | 3.9949e+5 (229) | 6.3800e+6 (486) | 1.0309e+8 (1040) |

Table 5: Preconditioners M_1^I , M_2^I and M_3^I ($N = 16$, $\alpha = 1$): condition number estimates and iteration counts. Piecewise linear discontinuous coarse space.

| Preconditioner M_1^I | | | | |
|------------------------------|-------------|-------------|--------------|--------------|
| $H \downarrow h \rightarrow$ | h_0 | $h_0/2$ | $h_0/4$ | $h_0/8$ |
| H_0 | 4.4817 (20) | 7.3013 (26) | 13.8371 (36) | 27.7972 (51) |
| $H_0/2$ | - | 4.7381 (21) | 7.8524 (28) | 14.4631 (38) |
| $H_0/4$ | - | - | 4.7748 (22) | 8.1640 (29) |
| $H_0/8$ | - | - | - | 4.9653 (23) |

| Preconditioner M_2^I | | | | |
|------------------------------|-------------|-------------|--------------|--------------|
| $H \downarrow h \rightarrow$ | h_0 | $h_0/2$ | $h_0/4$ | $h_0/8$ |
| H_0 | 5.9734 (24) | 9.7880 (31) | 18.2750 (42) | 36.4445 (58) |
| $H_0/2$ | - | 6.4031 (26) | 10.4022 (34) | 18.9555 (45) |
| $H_0/4$ | - | - | 6.6069 (28) | 10.7379 (35) |
| $H_0/8$ | - | - | - | 6.5152 (28) |

| Preconditioner M_3^I | | | | |
|--|-----------------|-----------------|-----------------|------------------|
| $H \downarrow h \rightarrow$ | h_0 | $h_0/2$ | $h_0/4$ | $h_0/8$ |
| H_0 | 6.0084 (24) | 9.8017 (31) | 18.2784 (42) | 36.4448 (58) |
| $H_0/2$ | - | 6.4362 (27) | 10.4172 (34) | 18.9593 (45) |
| $H_0/4$ | - | - | 6.6491 (28) | 10.7544 (34) |
| $H_0/8$ | - | - | - | 6.5739 (28) |
| $\mathbb{B}_h^{-1/2} \mathbb{A}_h \mathbb{B}_h^{-1/2}$ | 1.2229e+2 (52) | 4.7212e+2 (100) | 1.8726e+3 (202) | 7.4752e+3 (410) |
| \mathbb{A}_h | 2.5173e+4 (115) | 3.9949e+5 (229) | 6.3800e+6 (486) | 1.0309e+8 (1040) |

Table 6: Preconditioners M_1^I , M_2^I and M_3^I ($N = 4$, $\alpha = 1$): condition number estimates and iteration counts. Piecewise linear discontinuous coarse space.

| Preconditioner M_1^I | | | | |
|------------------------------|--------------|--------------|--------------|---------------|
| $H \downarrow h \rightarrow$ | h_0 | $h_0/2$ | $h_0/4$ | $h_0/8$ |
| H_0 | 10.6099 (29) | 24.6977(43) | 54.5351 (63) | 114.8625 (91) |
| $H_0/2$ | - | 12.2398 (34) | 26.7205 (49) | 56.2146 (71) |
| $H_0/4$ | - | - | 13.2809 (37) | 28.0078 (51) |
| $H_0/8$ | - | - | - | 14.0256 (38) |

| Preconditioner M_2^I | | | | |
|--|-----------------|-----------------|-----------------|------------------|
| $H \downarrow h \rightarrow$ | h_0 | $h_0/2$ | $h_0/4$ | $h_0/8$ |
| H_0 | 12.0117 (31) | 28.4619 (46) | 62.7619 (67) | 132.3684 (95) |
| $H_0/2$ | - | 14.0306 (36) | 30.7275 (52) | 64.7140 (74) |
| $H_0/4$ | - | - | 15.1082 (40) | 31.8235 (55) |
| $H_0/8$ | - | - | - | 15.8052 (42) |
| $\mathbb{B}_h^{-1/2} \mathbb{A}_h \mathbb{B}_h^{-1/2}$ | 1.2229e+2 (52) | 4.7212e+2 (100) | 1.8726e+3 (202) | 7.4752e+3 (410) |
| \mathbb{A}_h | 2.5173e+4 (115) | 3.9949e+5 (229) | 6.3800e+6 (486) | 1.0309e+8 (1040) |

Table 7: Preconditioners M_1^I and M_2^I ($N = 16$, $\alpha = 1$): condition number estimates and iteration counts. Piecewise constant discontinuous coarse space.

5.3 Variable penalty parameter

The aim of this section is to validate the independence on the penalty parameter α of the estimates for the condition number of the preconditioned system proved in Theorem 4.1.

For the sake of brevity we focus only on the performance of the preconditioners \mathbb{M}_1^E and \mathbb{M}_1^I , additionally throughout this section we employ a piecewise constant coarse solver. In Figure 5.3 we report the condition number estimates of the preconditioned system for different values of α . Although our theory requires $\alpha \geq 1$ for the sake of completeness we report here the results obtained with $\alpha = 10^{-2}, \dots, 10^4$, and different mesh configurations. Results obtained with exact local solvers, i.e., the preconditioner \mathbb{M}_1^E , are shown in Figure 3(a), whereas Figure 3(b) shows the analogous results obtained with inexact local solvers, i.e., the preconditioner \mathbb{M}_1^I . As expected, our preconditioner is fairly insensitive on the choice of the penalization constant.

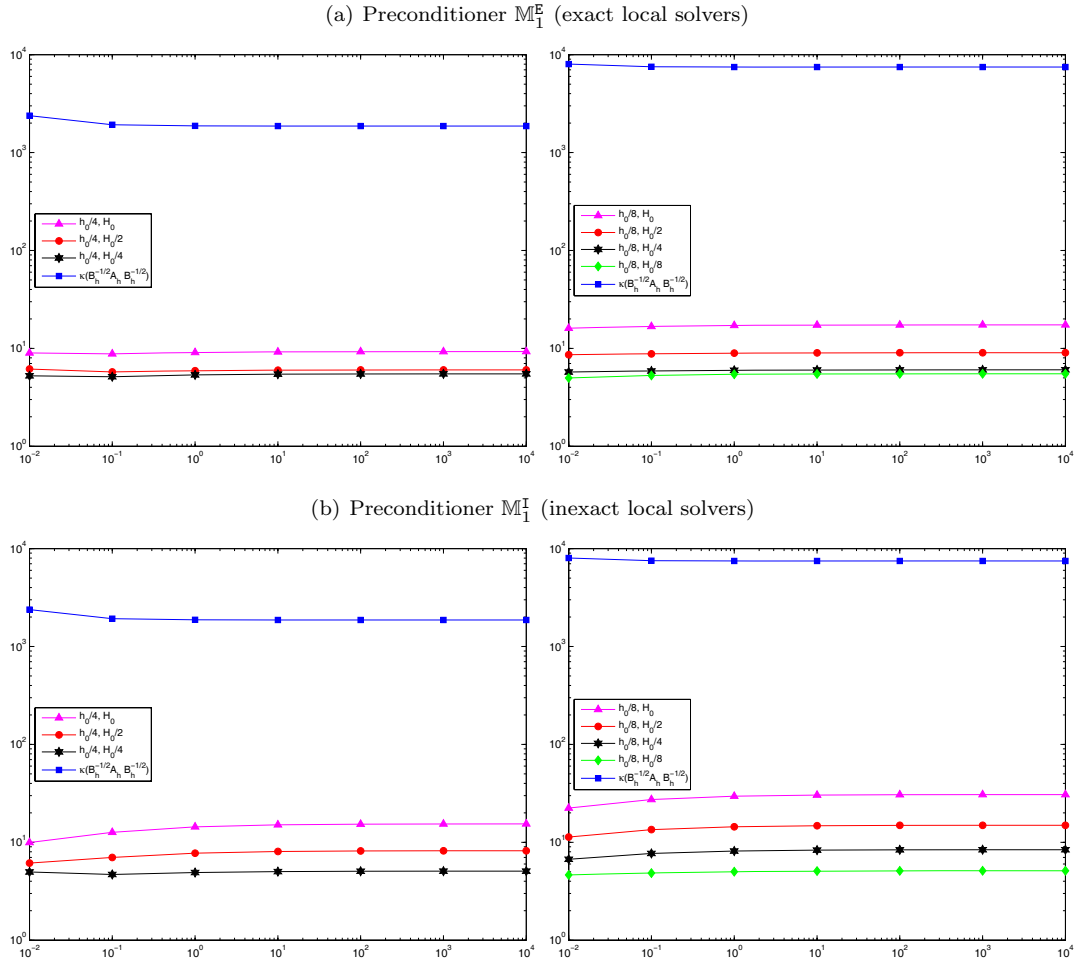


Figure 4: Preconditioners \mathbb{M}_1^E and \mathbb{M}_1^I ($N = 16$): condition number estimates as a function of the penalty parameter α . Piecewise constant coarse solver.

Acknowledgments

The work of P.F. Antonietti and B. Ayuso de Dios was partially supported by *Azioni Integrate Italia-Spagna* through the projects IT097ABB10 and HI2008-0173. B. Ayuso de Dios was also partially supported by MEC through the grant MTM2008 – 03541. The work of S.C. Brenner and L.-Y. Sung was supported in part by the National Science Foundation under Grant DMS-10-16332.

A Appendix

The aim of this section is to show Lemma 2.1. For that purpose, we first recall a result that provides a natural splitting of the DG linear functions.

Proposition A.1. [5, Proposition 3.1] *For any $u \in V_h$ there exist a unique $v \in V_h^{CR}$ and a unique $z \in \mathcal{Z}_h$ such that $u = v + z$. That is: $V_h = V_h^{CR} \oplus \mathcal{Z}_h$, where V_h^{CR} is the classical Crouziex-Raviart space defined by*

$$V_h^{CR} := \{v \in L^2(\Omega) : v|_T \in \mathbb{P}^1(T) \quad \forall T \in \mathcal{T}_h \quad \text{and} \quad \Pi_e^0(\llbracket v \rrbracket) = 0 \quad \forall e \in \mathcal{E}_h^\circ\}.$$

and the space \mathcal{Z}_h is defined by:

$$\mathcal{Z}_h := \{v \in L^2(\Omega) : v|_T \in \mathbb{P}^1(T) \quad \forall T \in \mathcal{T}_h \quad \text{and} \quad \Pi_e^0(\llbracket v \rrbracket) = 0 \quad \forall e \in \mathcal{E}_h^\circ\}.$$

A natural set of basis functions associated to midpoints of edges can be given for both spaces V_h^{CR} and \mathcal{Z}_h , i.e.,

$$V_h^{CR} = \text{span}\{\varphi_e^{CR}\}_{e \in \mathcal{E}_h^\circ} \quad \mathcal{Z}_h = \text{span}\{\psi_{e,T}^{\mathcal{Z}_h}\}_{e \in \mathcal{E}_h^\circ} \oplus \text{span}\{\psi_{e,T}^{\mathcal{Z}_h}\}_{e \in \mathcal{E}_h^\partial}. \quad (56)$$

Therefore, an edgewise ordering of the dofs of any $u \in V_h$ facilitates the use of the above splitting.

For any $u \in V_h$, let $v \in V_h^{CR}$ and $z \in \mathcal{Z}_h$ such that $u = v + z$. Now, we fix an interior edge $e = \partial T^+ \cap \partial T^-$, $e \in \mathcal{E}_h^\circ$ and, we denote by \mathbf{v}_e (resp. \mathbf{z}_e) the vector containing the degrees of freedom of $v|_{e \cap T^+}$ and $v|_{e \cap T^-}$ (resp. $z|_{e \cap T^+}$ and $z|_{e \cap T^-}$). Using the definition of the spaces V_h^{CR} and \mathcal{Z}_h , it follows that,

$$\mathbf{v}_e = \begin{bmatrix} v_e \\ v_e \end{bmatrix}, \quad \mathbf{z}_e = \begin{bmatrix} |z_e| \\ -|z_e| \end{bmatrix}, \quad \mathbf{u}_e = \begin{bmatrix} u^+ \\ u^- \end{bmatrix} = \begin{bmatrix} v_e + |z_e| \\ v_e - |z_e| \end{bmatrix} = \mathbf{v}_e + \mathbf{z}_e,$$

Therefore, we have that

$$(\mathbb{B}_h^e)^{-1/2} \mathbf{u}_e = \begin{bmatrix} v_e + \beta_e |z_e| \\ v_e - \beta_e |z_e| \end{bmatrix} = \mathbf{v}_e + \beta_e \mathbf{z}_e \quad \forall e \in \mathcal{E}_h^\circ,$$

where β_e is defined as in (8). Therefore, with such a decomposition the action of the operator $(\mathbb{B}_h^e)^{-1/2}$ can be read as the one that, on each interior edge, leaves untouched the Crouziex-Raviart part of the DG function and acts only on its highly oscillatory component z . Analogously, on each boundary edge $e \in \mathcal{E}_h^\partial$, we have

$$(\mathbb{B}_h^e)^{-1/2} \mathbb{Q}^T \mathbf{u}_e = \beta_e^\partial \mathbf{z}_e \quad \forall e \in \mathcal{E}_h^\partial,$$

where, following [5], we have assigned the dofs corresponding to the boundary edges (of the Dirichlet problem) in \mathcal{Z}_h (or, analogously, the Dirichlet boundary conditions with Crouzeix-Raviart elements are imposed strongly). Summarizing, we have

$$(\mathbb{B}_h^e)^{-1/2} \mathbf{u}_e = \begin{cases} \mathbf{v}_e + \beta_e \mathbf{z}_e & \text{if } e \in \mathcal{E}_h^\circ, \\ \beta_e \mathbf{z}_e & \text{if } e \in \mathcal{E}_h^\partial, \end{cases} \quad (57)$$

where β_e is defined in (8).

We also recall the following result from [5]. We report the proof for the sake of completeness.

Lemma A.2. For any $z \in \mathcal{Z}_h$ it holds that

$$\sum_{T \in \mathcal{T}_h} \|\nabla z\|_{0,T}^2 \leq C_t^2 \sum_{e \in \mathcal{E}_h} \frac{1}{h_e} \|\Pi_0^e(\llbracket z \rrbracket)\|_{0,e}^2, \quad (58)$$

where C_t is the constant in the trace inequality (and so depends only on the shape regularity of the mesh).

Proof. Integrating by parts, recalling that since $z \in \mathcal{Z}_h$ is piecewise linear then $\Delta z = 0$ on each $T \in \mathcal{T}_h$, and the definition (4) of the operator $\Pi_0^e(\cdot)$ yield

$$\begin{aligned} \sum_{T \in \mathcal{T}_h} \|\nabla z\|_{0,T}^2 &= (\nabla z, \nabla z)_{0,T} = - \sum_{T \in \mathcal{T}_h} \int_T \Delta z z \, dx + \sum_{e \in \mathcal{E}_h} \int_e \{\{\nabla z\}\} \cdot \llbracket z \rrbracket \, ds + \sum_{e \in \mathcal{E}_h^\circ} \int_e \llbracket \nabla z \rrbracket \cdot \{\{z\}\} \, ds \\ &= \sum_{e \in \mathcal{E}_h} \int_e \{\{\nabla z\}\} \cdot \Pi_0^e(\llbracket z \rrbracket) \, ds + \sum_{e \in \mathcal{E}_h^\circ} \int_e \llbracket \nabla z \rrbracket \cdot \Pi_0^e(\{\{z\}\}) \, ds \\ &= \sum_{e \in \mathcal{E}_h} \int_e \{\{\nabla z\}\} \cdot \Pi_0^e(\llbracket z \rrbracket) \, ds \\ &\leq \sum_{e \in \mathcal{E}_h} h_e^{1/2} \|\{\{\nabla z\}\}\|_{0,e} h_e^{-1/2} \|\Pi_0^e(\llbracket z \rrbracket)\|_{0,e}. \end{aligned}$$

The thesis follows by employing the standard trace inequality. \square

Finally, we are ready to prove Lemma 2.1.

Proof of Lemma 2.1. From the decomposition of the space V_h given in Proposition A.1, any $u \in V_h$ can be decomposed uniquely as $u = u^{cr} + u^z$, with $u^{cr} \in V_h^{CR}$ and $u^z \in \mathcal{Z}_h$. Recalling now that $B_h^{-1/2}u = u^{cr} + \beta u^z$, with $\beta|_e = \beta_e$ defined as in (8), we find

$$\begin{aligned} \sum_{e \in \mathcal{E}_h} \frac{\alpha}{h_e^3} \|\Pi^0(\llbracket B_h^{-1/2}u \rrbracket)\|_{0,e}^2 &= \sum_{e \in \mathcal{E}_h} \frac{\alpha}{h_e^3} \|\Pi^0(\llbracket u^{cr} + \beta_e u^z \rrbracket)\|_{0,e}^2 = \sum_{e \in \mathcal{E}_h} \beta_e^2 \frac{\alpha}{h_e^3} \|\Pi^0(\llbracket u^z \rrbracket)\|_{0,e}^2 \\ &\leq \sum_{e \in \mathcal{E}_h} \frac{1}{h_e} \|\Pi^0(\llbracket u \rrbracket)\|_{0,e}^2, \end{aligned}$$

where the last bound follows from estimate (9). We now show the continuity (16). For any $u, w \in V_h$, we write $u = u^{cr} + u^z$ and $w = w^{cr} + w^z$ with $u^{cr}, w^{cr} \in V_h^{CR}$ and $u^z, w^z \in \mathcal{Z}_h$. Then, the Cauchy-Schwarz inequality and the above inequality, gives

$$\begin{aligned} \mathcal{D}_h(u, w) &\leq \left(\sum_{T \in \mathcal{T}_h} \|\nabla(u^{cr} + \beta u^z)\|_{0,T}^2 \right)^{1/2} \left(\sum_{T \in \mathcal{T}_h} \|\nabla(w^{cr} + \beta w^z)\|_{0,T}^2 \right)^{1/2} \\ &\quad + \left(\sum_{e \in \mathcal{E}_h} \frac{1}{h_e} \|\Pi^0(\llbracket u \rrbracket)\|_{0,e}^2 \right)^{1/2} \left(\sum_{e \in \mathcal{E}_h} \frac{1}{h_e} \|\Pi^0(\llbracket w \rrbracket)\|_{0,e}^2 \right)^{1/2}. \quad (59) \end{aligned}$$

We now estimate each term on the right hand side separately (it is enough to do this for $u = u^{cr} + u^z$). The triangle inequality, the arithmetic-geometric inequality together with Lemma A.2, and the definition (8) of β yield the estimate

$$\sum_{T \in \mathcal{T}_h} \|\nabla(u^{cr} + \beta u^z)\|_{0,T}^2 \lesssim \sum_{T \in \mathcal{T}_h} (\|\nabla u^{cr}\|_{0,T}^2 + \beta^2 \|\nabla u^z\|_{0,T}^2)$$

$$\begin{aligned}
&= \sum_{T \in \mathcal{T}_h} (\|\nabla(u^{cr} + u^z - u^z)\|_{0,T}^2 + \beta^2 \|\nabla u^z\|_{0,T}^2) \\
&\lesssim \sum_{T \in \mathcal{T}_h} \|\nabla(u^{cr} + u^z)\|_{0,T}^2 + \sum_{e \in \mathcal{E}_h} \frac{(1 + \beta_e^2)}{h_e} \|\Pi_0^e(\llbracket u^z \rrbracket)\|_{0,e}^2 \\
&\lesssim \sum_{T \in \mathcal{T}_h} \|\nabla u\|_{0,T}^2 + \sum_{e \in \mathcal{E}_h} \frac{1}{h_e} \|\Pi_0^e(\llbracket u \rrbracket)\|_{0,e}^2.
\end{aligned} \tag{60}$$

which yields (16).

We now prove the coercivity. Cauchy-Schwarz inequality, the arithmetic-geometric inequality and estimate (58) from Lemma A.2 imply

$$\begin{aligned}
2 \left| \int_{\Omega} \beta \nabla_h u^{cr} \cdot \nabla_h u^z \, dx \right| &\leq 2 \|\beta \nabla_h u^{cr}\|_{0,\Omega} \|\nabla_h u^z\|_{0,\Omega} \\
&\leq 8C_t^2 \beta^2 \|\nabla_h u^{cr}\|_{0,\Omega}^2 + \frac{1}{8C_t^2} \|\nabla_h u^z\|_{0,\Omega}^2, \\
&\leq 8C_t^2 \beta^2 \|\nabla_h u^{cr}\|_{0,\Omega}^2 + \frac{1}{8} \sum_{e \in \mathcal{E}_h} \frac{1}{h_e} \|\Pi_0(\llbracket u^z \rrbracket)\|_{0,e}^2,
\end{aligned}$$

where C_t denotes the constant for the trace inequality. The above estimate together with the scaling of β_e given in (9) and the assumption $\alpha \geq 1$ yield

$$\frac{1}{h_e} \geq \beta_e^2 \frac{\alpha}{h_e^3} = \frac{\alpha}{h_e} \left(\frac{1}{k\alpha + h_e^2} \right) \geq \frac{\alpha}{h_e} \left(\frac{1}{k\alpha + 1} \right) \geq \frac{1}{2kh_e} \geq \frac{1}{4h_e},$$

with $k = 1$ if $e \in \mathcal{E}_h^\circ$ and $k = 2$ if $e \in \mathcal{E}_h^\partial$. The above observations together with Lemma A.2 finally give

$$\begin{aligned}
\mathcal{D}_h(u, u) &\geq \|\nabla_h u^{cr}\|_{0,\Omega}^2 + \beta^2 \|\nabla_h u^z\|_{0,\Omega}^2 + \sum_{e \in \mathcal{E}_h} \beta_e^2 \frac{\alpha}{h_e^3} \|\Pi_0^e(\llbracket u^z \rrbracket)\|_{0,e}^2 - 2\beta \left| \int_{\Omega} \nabla_h u^{cr} \cdot \nabla_h u^z \, dx \right| \\
&\gtrsim (1 - 8C_t^2 \beta^2) \|\nabla_h u^{cr}\|_{0,\Omega}^2 + \beta^2 \|\nabla_h u^z\|_{0,\Omega}^2 + \left(\frac{1}{4} - \frac{1}{8} \right) \sum_{e \in \mathcal{E}_h} \frac{1}{h_e} \|\Pi_0(\llbracket u^z \rrbracket)\|_{0,e}^2 \\
&\gtrsim (1 - 8C_t^2 \beta^2) \|\nabla_h u^{cr}\|_{0,\Omega}^2 + \beta^2 \|\nabla_h u^z\|_{0,\Omega}^2 + \sum_{e \in \mathcal{E}_h} \frac{1}{8h_e} \|\Pi_0(\llbracket u \rrbracket)\|_{0,e}^2.
\end{aligned}$$

Hence, by taking h so that $1 - 8C_t^2 \beta^2 \geq 1/2 > 0$, we have

$$\mathcal{D}_h(u, u) \geq \frac{1}{2} \|\nabla_h u^{cr}\|_{0,\Omega}^2 + \beta^2 \|u^z\|_{1,h}^2 + \sum_{e \in \mathcal{E}_h} \frac{1}{8h_e} \|\Pi_0(\llbracket u \rrbracket)\|_{0,e}^2,$$

and therefore, discarding the low order terms we finally obtain (because of Lemma A.2)

$$\mathcal{D}_h(u, u) \gtrsim \|\nabla_h u^{cr}\|_{0,\Omega}^2 + \sum_{e \in \mathcal{E}_h} \frac{1}{8h_e} \|\Pi_0(\llbracket u \rrbracket)\|_{0,e}^2 \gtrsim \|u\|_{\text{DG}}^2$$

for all $h \leq \sqrt{\frac{2\alpha}{16C_t^2 - 1}}$ and the proof is complete. \square

References

- [1] R. A. Adams. *Sobolev spaces*. Academic Press [A subsidiary of Harcourt Brace Jovanovich, Publishers], New York-London, 1975. Pure and Applied Mathematics, Vol. 65.
- [2] P. F. Antonietti and B. Ayuso. Schwarz domain decomposition preconditioners for discontinuous Galerkin approximations of elliptic problems: non-overlapping case. *M2AN Math. Model. Numer. Anal.*, 41(1):21–54, 2007.
- [3] P. F. Antonietti and B. Ayuso. Multiplicative Schwarz methods for discontinuous Galerkin approximations of elliptic problems. *M2AN Math. Model. Numer. Anal.*, 42(3):443–469, 2008.
- [4] D. N. Arnold, F. Brezzi, B. Cockburn, and L. D. Marini. Unified analysis of discontinuous Galerkin methods for elliptic problems. *SIAM J. Numer. Anal.*, 39(5):1749–1779 (electronic), 2001/02.
- [5] B. Ayuso and L. T. Zikatanov. Uniformly convergent iterative methods for discontinuous galerkin discretizations. *J. Sci. Comput.*, 40(1–3):4–36, 2009.
- [6] A. T. Barker, S. C. Brenner, E.-H. Park, and L.-Y. Sung. Two-level additive Schwarz preconditioners for a weakly over-penalized symmetric interior penalty method. *J. Sci. Comput.*, 47:27–49, 2011.
- [7] S. C. Brenner. Poincaré-Friedrichs inequalities for piecewise H^1 functions. *SIAM J. Numer. Anal.*, 41(1):306–324 (electronic), 2003.
- [8] S. C. Brenner, T. Gudi, L. Owens, and L.-Y. Sung. An intrinsically parallel finite element method. *J. Sci. Comput.*, 42(1):118–121, 2010.
- [9] S. C. Brenner and L. Owens. A weakly over-penalized non-symmetric interior penalty method. *JNAIAM J. Numer. Anal. Ind. Appl. Math.*, 2(1-2):35–48, 2007.
- [10] S. C. Brenner, L. Owens, and L.-Y. Sung. A weakly over-penalized symmetric interior penalty method. *Electron. Trans. Numer. Anal.*, 30:107–127, 2008.
- [11] S. C. Brenner, L. Owens, and L.-Y. Sung. Higher order over-penalized symmetric interior penalty methods. *preprint*, 2011.
- [12] S. C. Brenner and L. R. Scott. *The Mathematical Theory of Finite Element Methods (Third Edition)*. Springer-Verlag, New York, 2008.
- [13] M. Dryja and O. B. Widlund. Some domain decomposition algorithms for elliptic problems. In *Iterative methods for large linear systems (Austin, TX, 1988)*, pages 273–291. Academic Press, Boston, MA, 1990.
- [14] M. Dryja and O. B. Widlund. Towards a unified theory of domain decomposition algorithms for elliptic problems. In *Third International Symposium on Domain Decomposition Methods for Partial Differential Equations (Houston, TX, 1989)*, pages 3–21. SIAM, Philadelphia, PA, 1990.
- [15] X. Feng and O. A. Karakashian. Two-level additive Schwarz methods for a discontinuous Galerkin approximation of second order elliptic problems. *SIAM J. Numer. Anal.*, 39(4):1343–1365 (electronic), 2001.
- [16] A. Toselli and O. Widlund. *Domain decomposition methods—algorithms and theory*, volume 34 of *Springer Series in Computational Mathematics*. Springer-Verlag, Berlin, 2005.
- [17] T. Warburton and J. S. Hesthaven. On the constants in hp -finite element trace inverse inequalities. *Comput. Methods Appl. Mech. Engrg.*, 192(25):2765–2773, 2003.

MOX Technical Reports, last issues

Dipartimento di Matematica “F. Brioschi”,
Politecnico di Milano, Via Bonardi 9 - 20133 Milano (Italy)

- 39/2011** ANTONIETTI, P.F.; AYUSO DE DIOS, B.; BRENNER, S.C.; SUNG, L.-Y.
Schwarz methods for a preconditioned WOPSIP method for elliptic problems
- 38/2011** PORPORA A., ZUNINO P., VERGARA C., PICCINELLI M.
Numerical treatment of boundary conditions to replace lateral branches in haemodynamics
- 37/2011** IEVA, F.; PAGANONI, A.M.
Depth Measures For Multivariate Functional Data
- 36/2011** MOTAMED, M.; NOBILE, F.; TEMPONE, R.
A stochastic collocation method for the second order wave equation with a discontinuous random speed
- 35/2011** IAPICHINO, L.; QUARTERONI, A.; ROZZA, G.
A Reduced Basis Hybrid Method for the coupling of parametrized domains represented by fluidic networks
- 34/2011** BENACCHIO, T.; BONAVENTURA, L.
A spectral collocation method for the one dimensional shallow water equations on semi-infinite domains
- 33/2011** ANTONIETTI, P.F.; BEIRAO DA VEIGA, L.; LOVADINA, C.; VERANI, M.
Hierarchical a posteriori error estimators for the mimetic discretization of elliptic problems
- 32/2011** ALETTI, G.; GHIGLIETTI, A.; PAGANONI, A.
A modified randomly reinforced urn design
- 31/2011** ASTORINO, M.; BECERRA SAGREDO, J.; QUARTERONI, A.
A modular lattice Boltzmann solver for GPU computing processors
- 30/2011** NOBILE, F.; POZZOLI, M.; VERGARA, C.
Time accurate partitioned algorithms for the solution of fluid-structure interaction problems in haemodynamics